To: James W. Bales, Christina Silcox
From: Strobe 6: Adam Seering, Aubrey Tatarowicz, Daniel Hernandez, John Hawkinson
Date: 10 December 2008
Re: Breaking Glass Final Report
$Id: final.tex,v 1.59 2008/12/12 10:26:56 jhawk Exp jhawk $

1 Summary and Recommendations

This final project examined measurement of breaking glass using both high-speed video photography and sync-and-delay still photography. We experimented with a wide variety of ways to break the glass, and were able to produce quantitative measurements in several cases.

We began investigating glass breaking with thermal shock, moved to mild impact (falling weight), and ended up with high impact (BB rifle). We found the BB rifle produced the most reproducible and consistent results.

We examined both crack formation in the glass as well as deformation of the shape of the glass due to impact. We obtained useful data and used it to analyze the way shock waves move through glass. We found that the speed of the wave propagation and the crack formation were on the order of the speed of sound in glass.

We examined glass breaking using the Edgerton Center's Schlieren apparatus, but we did not discern any interesting optical properties with the Schlieren system.

We recommend that:

- We look into purchasing a faster high-speed video camera, such as the Phantom 12.1, that can take video at rates fast enough to capture at least 10-15 frames of glass cracking. The Phantom 12.1 can record at 1,000,000 fps (the current Phantom 7 is limited to 150,000 fps).
- We re-take video with this faster camera in order to get better time resolution in our measurements.
- We look into purchasing or creating software that can take two-dimensional images and turn them into three-dimensional representations, to better understand the deformation of the glass's surface.
- We repeat the tests involving glass deformation using this software.

Contents

2 Background

Our Mark 1 project determined what kinds of things we can see and measure with breaking glass. Our curiosity was piqued by rumor that car thieves break glass car windows by hitting them with a hot object. The combination of the impact and the thermal shock is allegedly sufficient to easily crack sturdy automotive glass.

In researching how we should go about breaking the glass and what we can measure, Dr. Bales referred us to a 2004 Strobe Lab group's report investigating some aspects of breaking glass [Bhuyan89]. This group investigated glass breaking by impact with a metal rod and also with a BB shot from a gun. The group recommended further study of thermal cracks. We wanted to do further work based on their research, including additional study of cracks due to thermal stress.

We want to use this information to get more useful data and also combine this with the thermal aspect of glass breaking. This group recommends a study on the thermal effects on glass breaking which is one of the things we wish to pursue.

2.1 Glass Breaking Process

Glass breaks when a stress fracture forms by some sort of stimulus, and this fracture travels though the glass until the glass breaks. This fracture speed has been studied in the past and is expected to be between 1000 m/s and 1500 m/s [Bhuyan89].

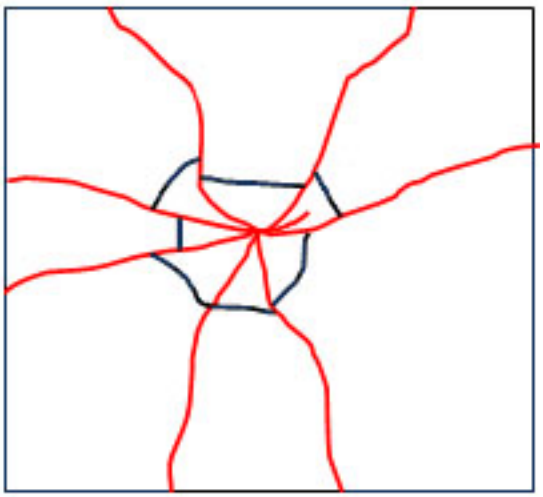

Figure 1: Concentric and radial fractures. The red lines are radial fractures. The black lines form a concentric fracture. [Jones02]

Fractures formed by impact take two distinct forms: radial fractures and concentric fractures. Radial fractures are considered primary fractures and form on initial impact. Concentric

fractures form around the point of impact. Figure 1 shows the two types of fracture patterns. The glass bends before breaking which causes these different shaped breaks [Bhuyan89]. We want to study how the glass bends.

2.2 Measuring Glass Fracture Speed

We used the high-speed video camera to measure glass fracture speed, and tested this technique in our Mark 1 project. This technique uses the frames captured by a high-speed video camera to take data, so that the movement of a fracture can be analyzed with respect to time [Ravi-Chandar]. We can do this analysis by hand by calibrating the image using an object of known size, like the length of the glass slide. With this data, we can extract position information and make velocity calculations. This is the same method as used in Lab 3 [IM3-JWB].

2.3 Seeing Glass Deformation — The Projected Grid Method

Glass deforms when it is struck by an object. One of our objectives is to capture this deformation on camera. One method explained to us by Dr. Bales is the "projected grid method." This method uses the idea that images look deformed when seen reflected off of an uneven surface. This is how funhouse mirrors work.

Using this idea, we can use light and a physical grid to project an image of the grid onto a glass surface. Then, we can position the camera to see the reflection of this grid. If or when the glass deforms, we can see this phenomenon captured by the camera because the projected grid will look deformed.

2.4 Bending of Material

The bending of materials is typically analyzed in terms of stress:

$$\rho = \frac{F}{A} \tag{1}$$

where ρ is the nominal-stress tensor, describing how stress is distributed throughout the beam. F is the force applied to the beam and A is the cross-sectional area of the beam.

Stress can be thought of as an internal pressure. Stress and pressure have the same units; "stress" is frequently used to describe solid objects where "pressure" would be used to

describe fluids.

Objects such as panes of glass seldom break due to linear forces; rather, they break due to the internal torques that cause them to bend. Rewriting the equation in terms of the torque M on the rod gives

$$\rho \cdot y = \frac{M}{A} \tag{2}$$

where $F = \frac{M}{y}$; y is the distance from the center plane of the beam to the point at which deflection is measured. If the stress of an object varies with position, such as with an object that is being bent, this equation can be rewritten as

$$M = \int_A \rho \cdot y dA \tag{3}$$

In most simple rods, ρ has been shown to be a simple constant. This makes this equation quite simple to work with.

2.5 High-Speed Video Camera — Phantom

The Phantom High-Speed Video camera is capable of recording 800×600 pixel video at 4,700 frames per second. It has a maximum frame rate of approximately 150,000 frames per second at a resolution of 32×32 pixels. This resolution and very high frame rate make it a versatile choice for capturing useful video of sudden or rapid events.

The Phantom connects to a control computer via Ethernet. The Phantom 640 software on the computer allows the user to modify the frame rate, resolution, shutter speed, and trigger settings for the camera. Once the video is captured, it can be reviewed, trimmed, and saved.

The Phantom captures data at a higher data rate than bulk recording devices, such as hard drives, can handle. As a result, it stores video in an on-board memory buffer. When triggered, it saves the state of the buffer, and it canthen send its contents off to a connected laptop. Once on the laptop, the video can be played back and converted to various data formats for analysis.

The Phantom can be triggered through the laptop's graphical user interface, or optionally through a separate external electrical trigger.

The Phantom responds to the trigger by continuing to capture a configurable number of frames after the trigger, anywhere from 1 frame to the entire capture buffer. Depending on

the circumstance, the camera can thus capture video prior to the trigger, or following the trigger, or somewhere in between.

2.6 Goals

Based on this information, our goals were:

- To evaluate breaking glass with thermal shock.
- To evaluate breaking glass with mild impact.
- To evaluate breaking glass with high impact.
- To obtain useful quantitative data about the breaking and shattering process.
- To evaluate the deformation of glass (prior to breaking), and collect quantitative and qualitative data about it.
- To measure the speed of crack propagation.
- To measure the speed of shock wave propagation.

3 Procedure

During this project we experimented with several different methodologies for breaking glass and measuring results. We broke small microscope slides, larger glass sheets, and mirrors in our six lab sessions. Tools used to break the glass included a heat gun, a screwdriver, and a BB gun. A high-speed video camera and a digital still camera captured the images, sometimes with the help of a beam-break trigger device. The procedures for the experiments are detailed in the following four sections.

3.1 Thermal Shock

For the tests of thermal shock, we used the materials listed in Table 1. The lab setup is as shown in Figures 2 and 3.

Table 1: Materials for thermal shock experiment.

Item	*Manufacturer*	*Model*	*S/N*
HSV camera	Vision Research	Phantom v7.1	Phantom HSV
Laptop computer	Dell	Latitude D830	MIT-0422773
HSV software	Vision Research	Phantom 640	DNR
Microscope slides	VWR International	$75 \times 25 \times 1$ mm	—
Digital multimeter	Fluke	179	93810559
Type K thermocouple	Fluke	—	—
Lens (for Phantom Camera)	Tamron	90 mm macro	TAMRON1
Digital Still Camera	Sony	DSC-P72	338694
Heat Gun	Accupro	1500 Watt	—
Tripod (for Phantom Camera)	Manfrotto	3021BPRO	—
Hex Plate for Tripod	—	—	—
Lamp	Lowel	Pro 250 W	—
Fiber Optic Illuminator	Dolan-Jenner Industries	190	—
Safety Glasses	DNR	DNR	—
Black Rolling Cart	—	—	—
Wooden Boxes (2)	—	—	—
Eyedropper	—	—	—
Titration device	DNR	DNR	—
Metal Lab Stands (2)	—	—	—
White Paper (for diffusion)	—	—	—
Water	—	tap water	—
Soldering iron	Weller	DNR	DNR

In our first test, we tried applying a soldering iron (with a tip temperature of around 150°C) to the microscope slide. Upon contact, the slide did not react. Upon extended contact, the slide continued to not react. We then removed the soldering iron and, after allowing the glass to cool, applied a second iron, with a higher tip temperature of around 250°C. Once again, the glass did not react. We measured all temperatures with the thermocouple.

In our second test, we tried heating the glass with a heat gun. We were able to heat the glass to about 375°C. This is much hotter than the soldering iron. However, the glass remained unaffected to the naked eye.

In our third test, we tried heating the glass with the heat gun, then dropping cold water on the glass to cool it rapidly. We tried a number of application methods, with varying results as discussed in the "Results" section. Specifically, we tested an eyedropper, a cup, and a titration device held at different heights relative to the glass.

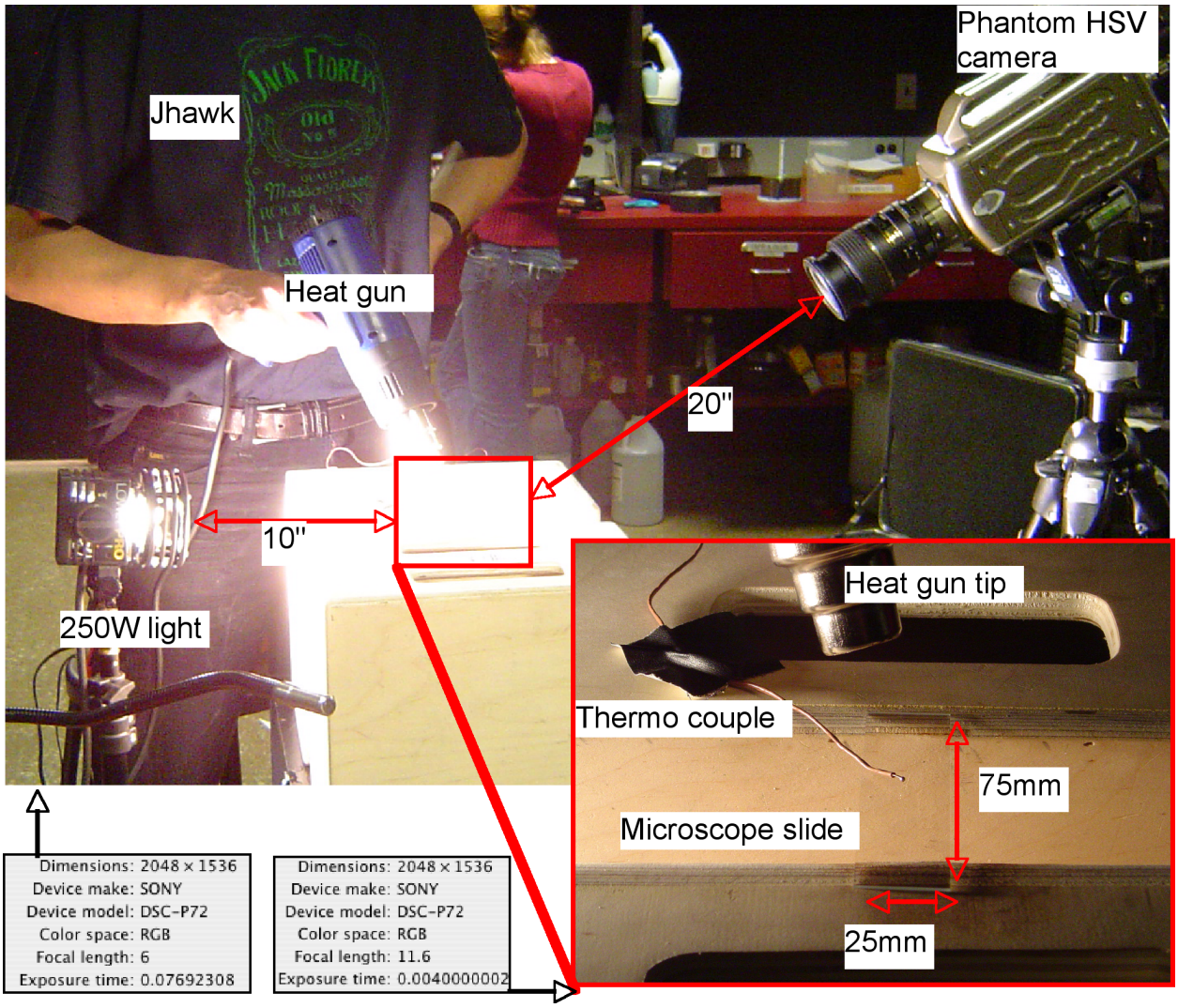

Figure 2: The first setup used to do the heat tests. We found that the apple boxes started to get singed by the applied heat from the heat gun, so the setup in Figure 3 is the setup we used. The lower image in the figure is a closer look at the setup of the microscope slide with the heat gun and thermocouple. The thermocouple is connected to the multimeter. The camera is about 45° above the slide. The 250 W light lights the far edge of the slide.

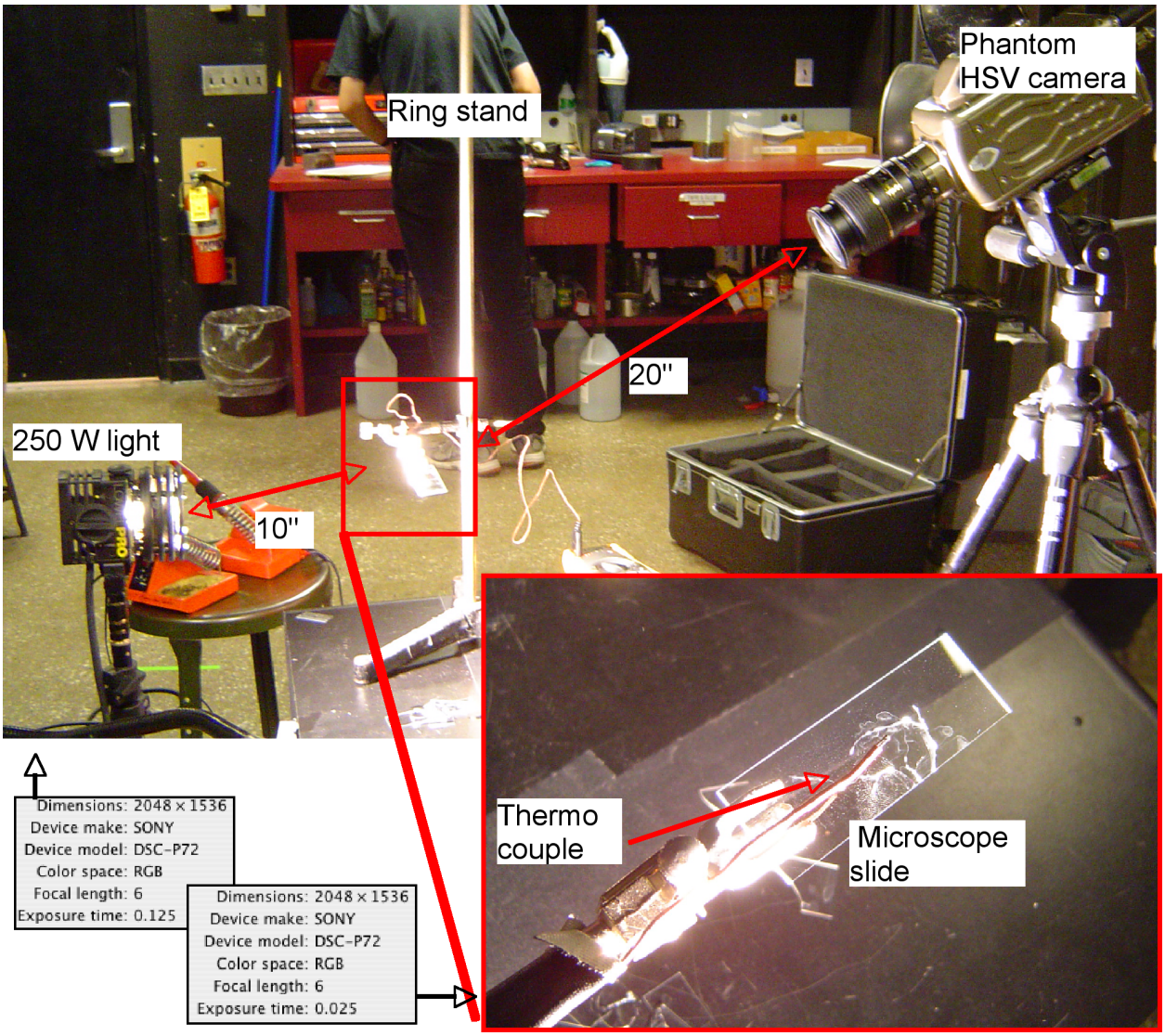

Figure 3: The setup we used for the thermal shock for most experiments. The clamp on the ring stand holds the microscope slide by one end as seen in the lower photo in this diagram. The light is aimed directly into the edge of the microscope slide opposite the camera.

3.1.1 Trigger Mechanisms

For testing different trigger mechanisms, we kept the setup from the heat-expansion experiments, and added a number of ring stands to support an optical trigger and a beam break trigger. The triggers were arranged as shown in Figure 4.

The optical trigger consists of an infrared LED spaced roughly 1 cm away from an infrared detector. The beam break trigger has a laser emitter and a detector that can be separated by several meters.

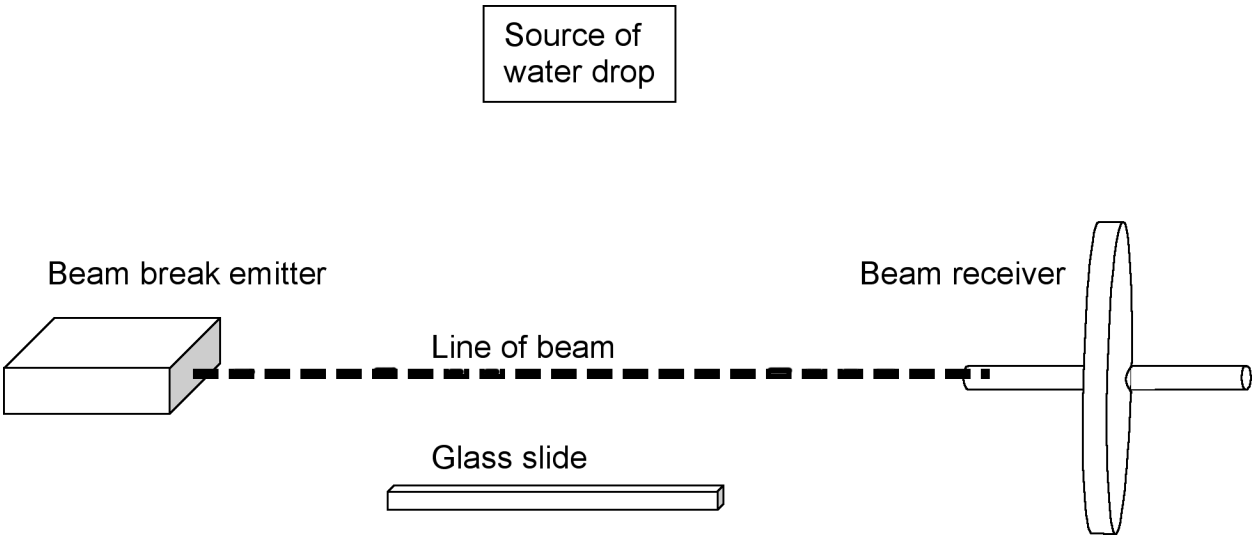

Figure 4: This is the basic beam break setup that we tried. The beam break components were secured in place with tape on lab stands and apple boxes until the beam was set so that the receiver lined up with the emitter and that the beam crossed over the glass slide and in the path of the water drop. The beam break trigger was connected to the Time Machine input, and the output of the time machine was connected to the Phantom HSV camera. The camera was set to trigger at the beginning of the recorded segment with the triggering from the beam break.

The goal was to have a drop of water pass through the beam of each trigger while airborne, prior to impacting the glass. We assumed that the water would fall in a very repeatable way, once released from its container. We tested for a successful trigger using the attached Time Machine device.

3.1.2 Lighting Techniques

Table 2: Materials for Lighting Experiment

Item	*Manufacturer*	*Model*	*S/N*
HSV camera	Vision Research	Phantom v7.1	Phantom HSV
Laptop computer	Dell	Latitude D830	MIT-0422773
HSV software	Vision Research	Phantom 640	DNR
Microscope slides	VWR International	$75 \times 25 \times 1$ mm	—
Digital Multimeter	Fluke	179	93810559
Type K thermocouple	Fluke	—	—
Lens (for Phantom Camera)	Nikon	28 mm	Nikon1
Digital P&S Camera	Sony	DSC-P72	338694
Tripod (for Phantom Camera)	Manfrotto	3021BPRO	—
Hex Plate for Tripod	—	—	—
Lamps (2)	Lowel	Pro 250 Watt	—
Lab stand (ring stand w/o ring)	—	—	—

For the tests of lighting techniques, we used the same camera setup as for testing thermal shock. We shifted the light around to test direct lighting, back-lighting, and side-lighting (where light is passed straight through the long edge of the glass, so that cracks will reflect the light and appear to glow). The equipment used is listed in Table 2.

These lighting setups were implemented as shown in Figure 5.

Additionally, we tried pointing the camera at the underside of slides rather than at the top.

We also looked into using digital still cameras to capture images of the glass. A camera could be used to take still images of the slide at a useful frame rate. However, because of the lack of a shutter release cable (for the Nikon D200), still photos of shattering glass were not attempted.

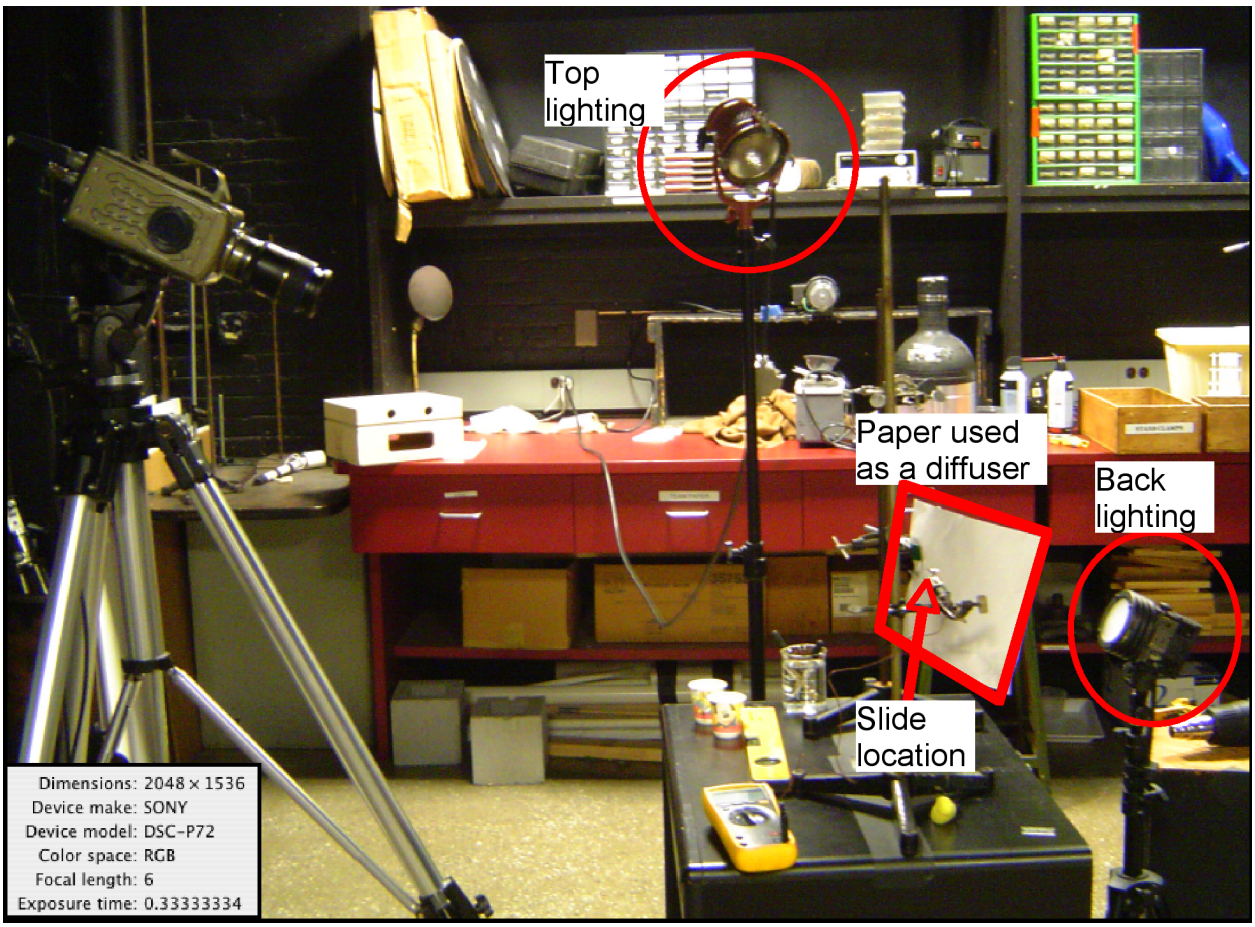

Figure 5: This figure shows the different lighting techniques we used. We used any combination of these techniques to obtain the results that we wanted. The paper diffuser was not used at all times and was helpful in some situations but not helpful in others.

3.2 Mild Impact

For the tests of glass impact, we set up a piece of glass suspended between two apple boxes, similar to the setup for testing thermal shock. The glass was then hit with a pendulum and a screwdriver, each from varying heights ranging from 1″ to 12″.

This procedure was followed with both 1 mm microscope glass and $^3/_{32}$″ window-pane class. We cut the window-pane glass into 2×8″ rectangular pieces.

The equipment used is listed in Table 3. The setup for this was as shown in Figure 6.

Table 3: Materials for glass impact experiment.

Item	*Manufacturer*	*Model*	*S/N*
HSV camera	Vision Research	Phantom v7.1	Phantom HSV
Laptop computer	Dell	Latitude D830	MIT-0422773
HSV software	Vision Research	Phantom 640	DNR
Microscope slides	VWR International	$75 \times 25 \times 1$ mm	—
Lens (for Phantom camera)	Nikon	28 mm	Nikon1
Digital P&S camera	Sony	DSC-P72	338694
Tripod (for Phantom camera)	Manfrotto	3021BPRO	—
Hex Plate for Tripod	—	—	—
Screwdriver	Craftsman	Flat head 41578	—
Glass	RF Supply	8″ x 10″ x $^3/_{32}$″	—
Lamps (2)	Lowel	Pro 250 Watt	—
Safety Glasses	—	—	—
Wooden Boxes (2)	—	—	—
Graph paper	DNR	—	—
Gaff tape	DNR	DNR	—

The object being dropped onto the glass was dropped once per test run listed in the "Results" section of this report, at a height above the glass as noted in Table 8. The glass either broke on impact, or did not break on impact.

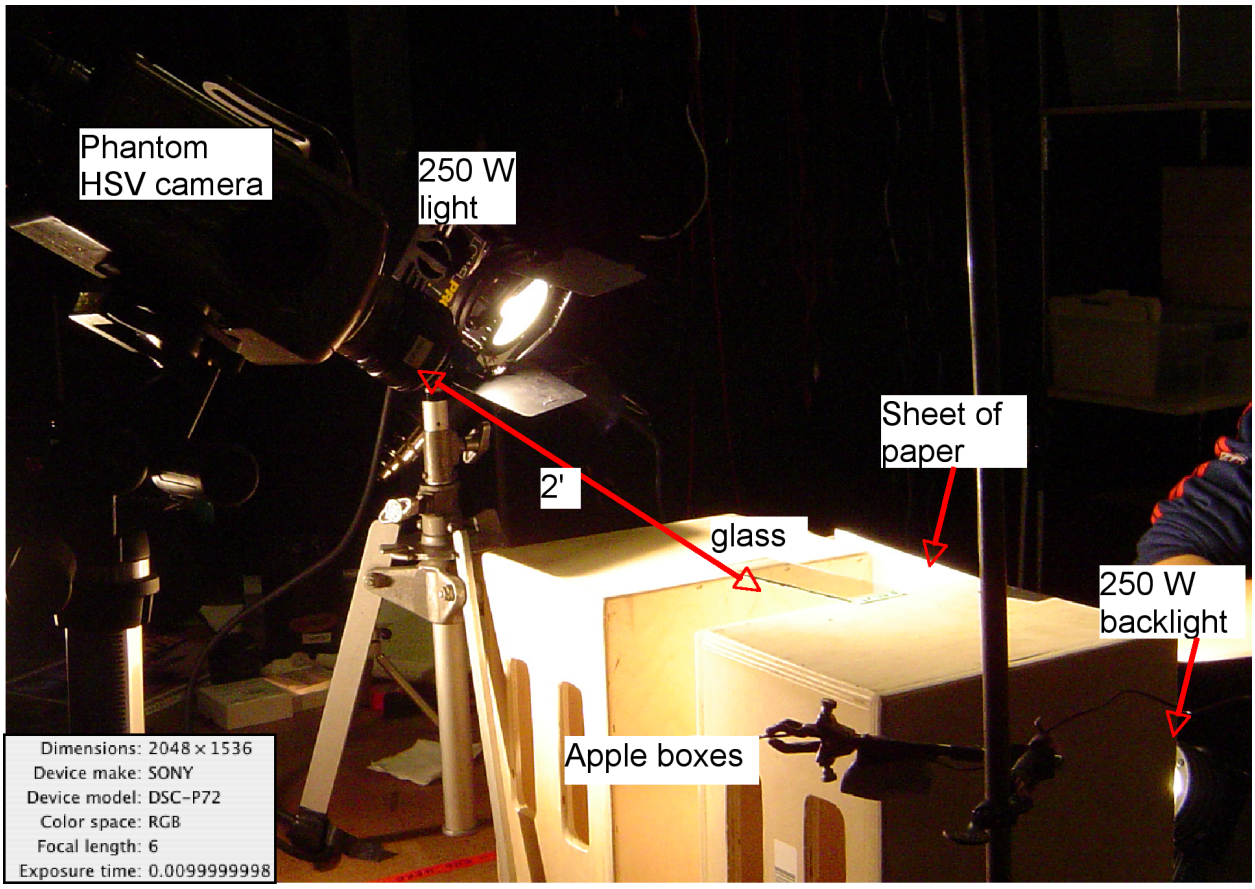

Figure 6: The setup used to perform the impact tests with the screwdriver. The glass is the $^3/_{32}''$ thick glass and the sheet is cut to $2 \times 8''$ and is secured with tape. The sheet of paper is suspended in front of the back light to diffuse the light going into the camera. The lens used is the 28 mm lens.

3.3 BB Rifle Fired at Glass Slides and Sheets

Table 4: List of equipment to conduct the following two sections in lab.

Item	*Manufacturer*	*Model*	*S/N*
BB rifle	Crossman Air Guns	760-C	188214595
Catalog	Digi-Key	—	—
Fiber optic illuminator	Dolan-Jenner	190	—
Lowel Pro light	Lowel	250 W	—
HSV camera	Vision Research	Phantom v7.1	Phantom HSV
Laptop computer	Dell	Latitude D830	MIT-0422773
HSV software	Vision Research	Phantom 640	DNR
50 mm lens	Nikon	50 mm	Nikon2
Tripod	Manfrotto	3058	A0747258
Apple boxes	—	—	—
Microscope slides	VWR International	$75 \times 25 \times 1$ mm	—
BBs (4.5 mm caliber)	Quick Silver	Match Grade No. 7541	—
Black wooden box	—	—	—
28 mm lens	Nikon	28 mm	Nikon1
Ring stand	—	—	—
Grid paper	—	—	—
Hex plate	—	—	—
Glass sheets	RF Supply	$8 \times 10 \times {}^{3}/_{32}''$	

The following two experiments (§3.3.1, §3.3.2) were conducted during the same lab session and were created by making slight alterations in the setup, making the equipment list the same. The first of these experiments is viewing crack formation on glass from BB impact. The second experiment was viewing glass deformation from BB impact.

3.3.1 Crack Formation

Table 4 outlines the equipment used to conduct this experiment. The purpose of this experiment was to see the crack formation on the glass during the process of a BB impact. Careful lighting was essential.

For both the glass sheets and the glass slides, the procedure was the same. For the diagrams for the glass slide setup refer to Figures 7 and 8. For the diagrams for the glass sheet setup, see to Figures 7 and 9.

In order to setup for these experiments, the glass was taped to the apple boxes on either end of the glass as shown in Figure 7. We positioned the book behind the glass and in the line of fire of the BB in order to catch the BBs. The Phantom was positioned so that the angle of incidence was about 45° with the glass. We aimed the BB rifle so that the BB hits the glass normal to the surface and in the center of the glass. A 250 W Lowel Pro lamp was

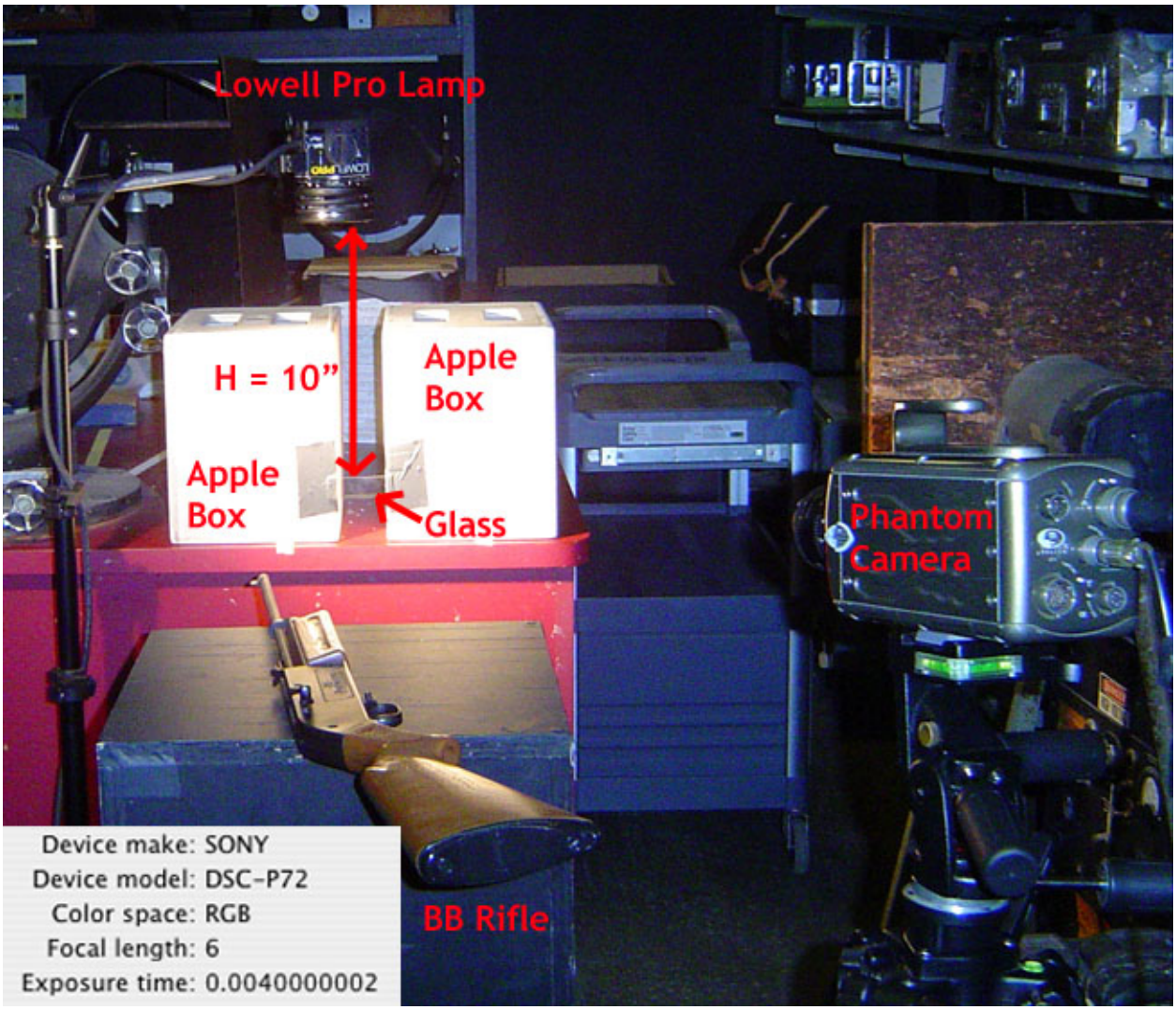

Figure 7: The view from the perspective of the gun holder of the setup used to capture the glass cracking from impact of a BB. This diagram is intended to show how the subject is lit in order to illuminate cracks. Figure 8 better illustrates all of the relative distances of the objects.

positioned directly above the glass and aimed down onto the glass edge. This was the only lighting except for the room's ambient light.

To set up the computer, we used the method described in the section 2, connecting the output of the Phantom camera to the Dell computer. The Phantom 640 software was opened in order to record the video from the Phantom camera and control the camera settings.

The most difficult task was this apparatus is getting the sync-and-delay to work so that the high-speed video captures the entire phenomenon. Since we were only capturing about one second of video with the frame rates we use for this test, careful timing was important. We found that using a beam break or sound trigger was fairly difficult, and it was sufficient to

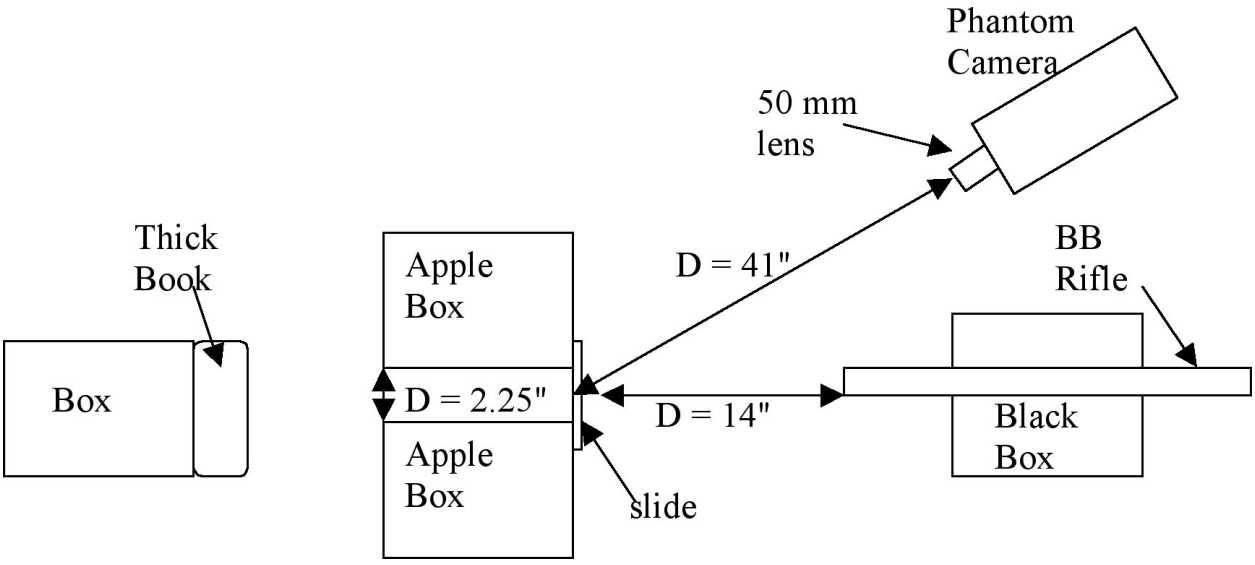

Figure 8: The bird's eye view of the diagram setup used to capture crack formation from BB impact on a glass slide. We used the 50 mm lens for this test, unlike the glass sheet trials. The thick book was taped to the box and was used to catch BBs. The slide was attached using tape as seen in Figure 7.

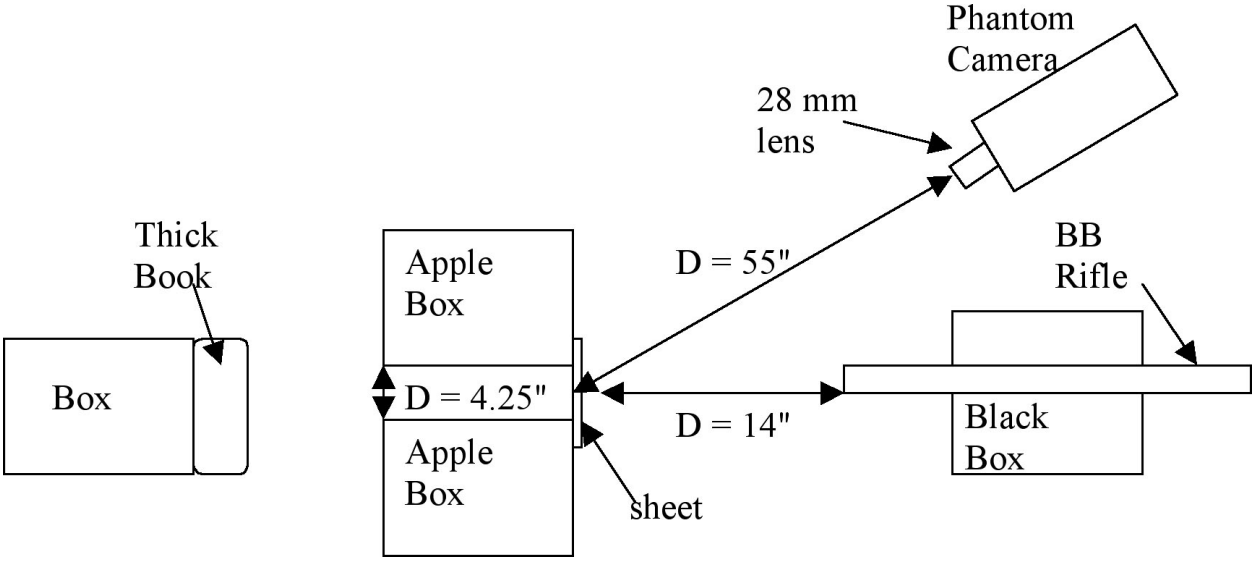

Figure 9: The bird's eye view of the diagram setup used to capture crack formation from BB impact on a glass sheet. This is very similar to Figure 8. The main changes that we needed to do for this setup was widen the apple box distance, change the lens to 28 mm, and change the camera-to-subject distance.

trigger manually. Using this method, we captured the glass breaking each time. We set up the trigger so that the frames captured after the trigger were saved.

We gave the BB gun the needed number of pumps, and then loaded the BB into the gun. Then, we made sure that the camera was set up with the correct parameters. From previous

tests, we knew we had to use a frame rate of around 75,000 fps, so that is what the camera was configured to. The aperture of the lens was adjusted between f/1.8 and f/4 in order to ensure enough light. The exact apertures used are in the results section.

Once the camera was ready to record, the shooter would aim the gun and turn the safety off. We would count down, and then fire the gun and trigger the Phantom simultaneously. Since the frames were saved after the trigger, we reliably captured the glass breaking.

3.3.2 Deformation with HSV — Our First Try

In order to view the deformation of glass from the impact of the BB, we added a projected grid to the previous setup. In doing so, we removed the light from above the glass sheet. The materials for this procedure can be found in Table 4. Figure 10 illustrates the basic setup used at this time to record glass deformation. Figure 11 shows how we projected the grid. In order to project the grid, we used a Lowell Pro 250 W lamp and placed grid paper in front of it. The light and grid setup were aimed at the glass. In order to see the deformation, we needed to focus on the grid projected onto the glass rather than the glass. We focused the camera so the reflected image of the grid was sharp. In order to capture the data, we used the same sync-and-delay method as in §3.3.1.

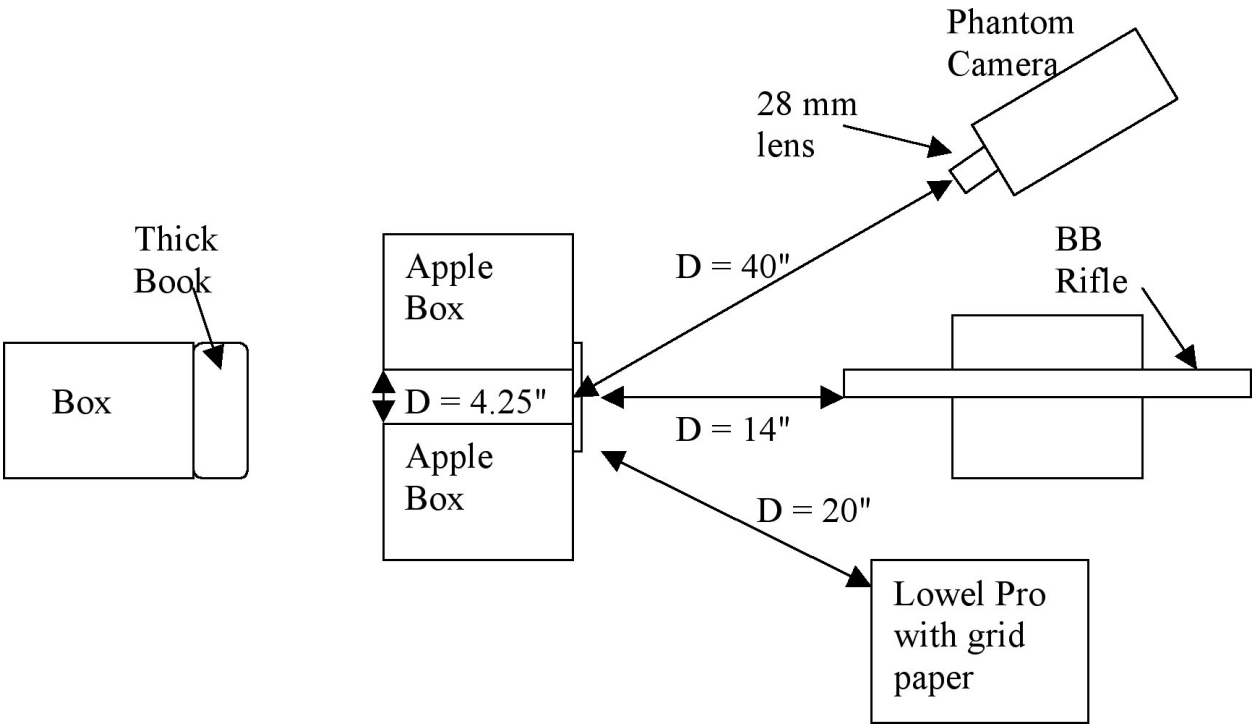

Figure 10: The bird's eye view of the diagram setup used to capture glass deformation as a result of the BB impact. This is similar to Figures 8 and 9, except the grid paper apparatus has been added. The grid paper apparatus can be seen in a close-up in Figure 11.

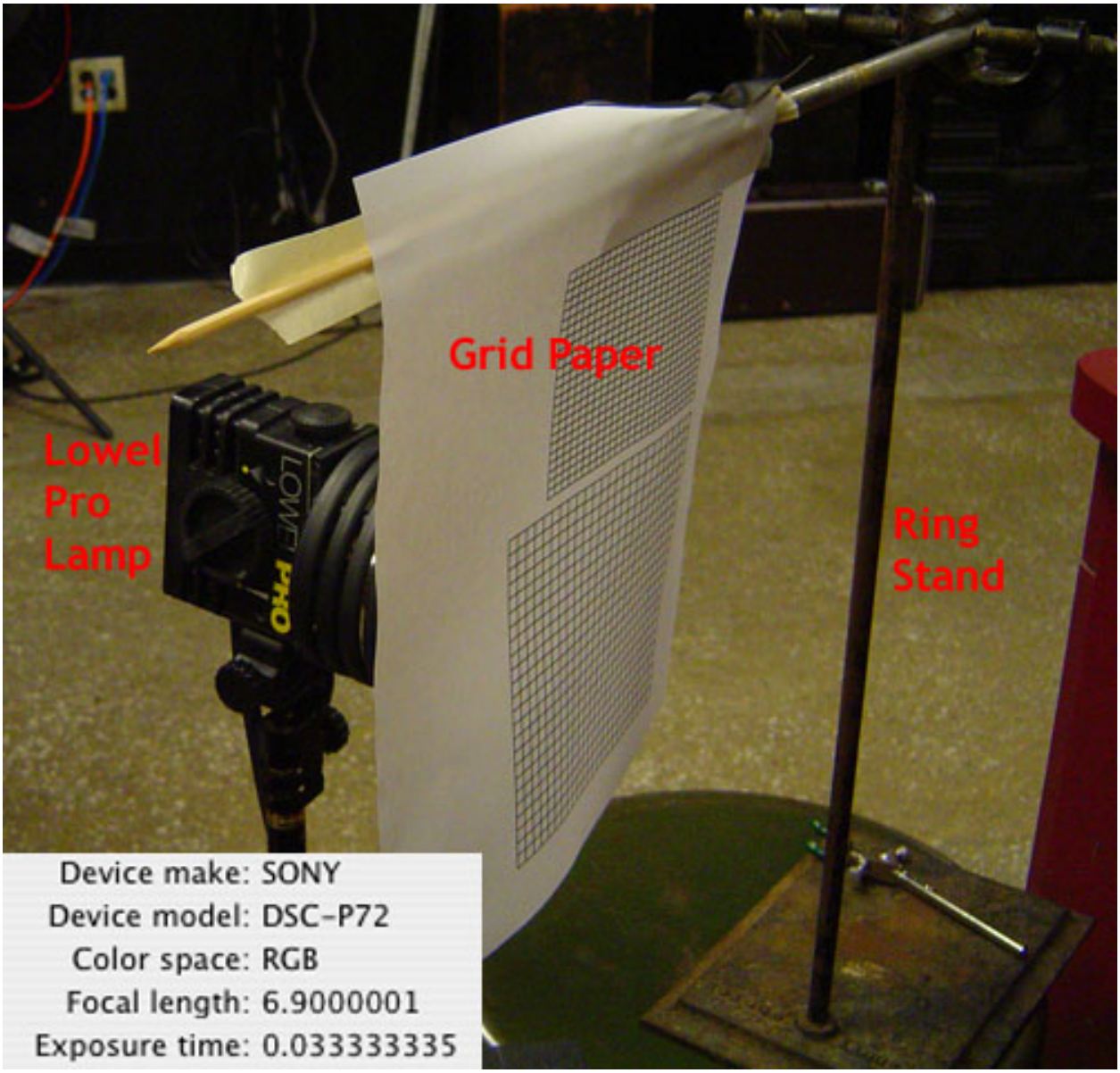

Figure 11: A figure of the method used to project the grid onto the glass for this high-speed camera setup. The grid paper is formed by printing a grid onto paper. The paper is held by taping it to a ring stand.

3.3.3 Deformation with HSV — Our Second Try

Table 5: Materials for Mirror and Grid Experiment

Item	*Manufacturer*	*Model*	*S/N*
HSV camera	Vision Research	Phantom v7.1	Phantom HSV
Laptop Computer	Dell	Latitude D830	MIT-0422773
HSV Software	Vision Research	Phantom 640	DNR
28 mm lens	Nikon	DNR	Nikon1
50 mm lens	Nikon	DNR	Nikon2
Digital Still Camera	Sony	DSC-P72	338694
Tripod	Manfrotto	3021BPRO	—
Hex Plate for Tripod	—	—	—
Lamp	Lowel	Pro 250 Watt	—
BB rifle	Crossman Air Guns	760-C	188214595
BBs (4.5 mm caliber)	Daisy	Match Grade No. 7541	—
Catalog	Digi-Key	DNR	—
First Surface Mirrors	American Science & Surplus	4112P1 $77 \times 194 \times 3$ mm	—
Glass	RF Supply	8 x 10 x $3/32''$	—
Ground Glass	American Science & Surplus	2728P6, $2 \times 2 \times 1/32''$	—
Wire grid	DNR	DNR	—
Lab stand	—	—	—
Ruler	—	—	—
Gaff tape	DNR	DNR	—
Wooden Boxes (2)	—	—	—
Tall wooden box for gun	—	—	—
Safety glasses	DNR	DNR	—

The experiment was set up as shown in Figure 12 using the materials listed in Table 5. The mirror was secured to the wooden boxes with tape. A thick catalog was placed behind the mirror to catch the discharged BBs. A section of wire mesh was clamped to a piece of ground glass and placed between the 250 W lamp and the mirror. The HSV camera was then angled to capture the projected image of the grid on the mirror. We started with the 28 mm lens and switched to the 50 mm lens for the higher resolution (320 x 240 pixels) videos.

The HSV camera was connected to the Dell computer via an Ethernet cable. The Phantom software was set to post-trigger, and as the shooter counted down, the person operating the computer would click the trigger button immediately before the shooter fired the BB gun. We ran several trials with the mirrors and the $3/32$" glass as well. We pumped the gun fewer times (to reduce the impact) for the glass trials since it was not as thick as the mirrors. The glass does not reflect as well as the mirrors, so we used a wider aperture. We also experimented with the expanded dynamic range (EDR) values in the Phantom software.

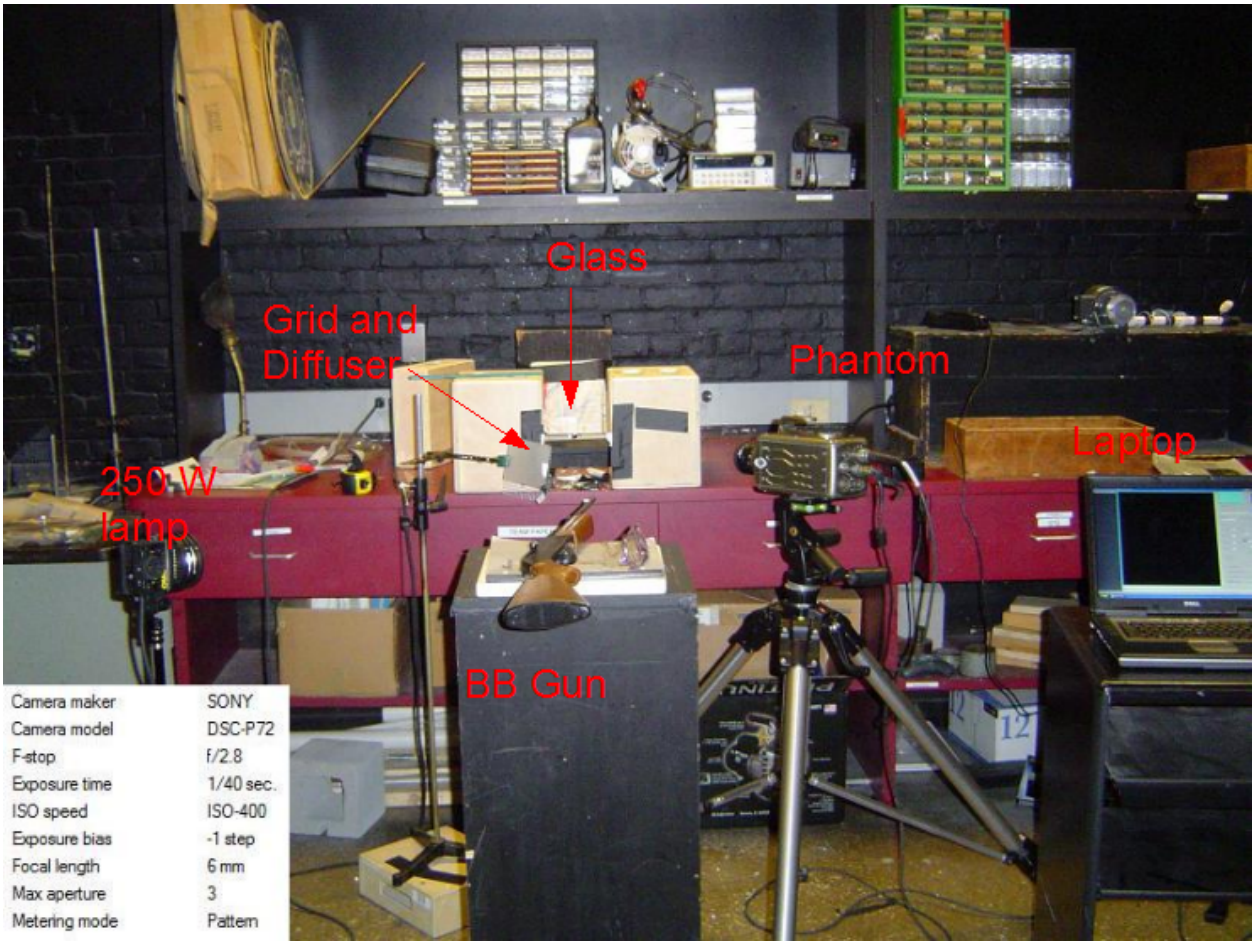

Figure 12: Setup for BB/grid experiment. The wire grid and ground glass are clamped and positioned between the 250 W lamp and the glass taped to the wooden boxes.

3.3.4 Deformation with Still Images

Table 6: Equipment used to conduct BB breaking glass with still images.

Item	*Manufacturer*	*Model*	*S/N*
BB rifle	Crossman Air Guns	760-C	188214595
BBs (4.5 mm caliber)	Quick Silver	Match Grade No. 7541	—
Catalog	Digi-Key	DNR	—
Lowel Pro light (250W)	Lowel	250 W	—
1 kW Halogen	DNR	DNR	—
Tripod	Manfrotto	3021B Pro	—
Apple boxes	—	—	—
Wooden spacer boxes	—	—	—
BB gun frame	—	—	—
DSLR camera	Nikon	D200	"D200"
Chicken wire	—	1 cm squares	—
Sheet of plexiglass	—	13"x13"	—
Tape	—	—	—
90 mm lens	Tamron	90 mm macro lens	Tamron1
SPOT	Prism Science Works	SPOT	Edgerton1
Time Machine	Mumford	"Time Machine"	Timer1
Trigger device	Mumford	beam break	DNR

In order to capture the glass deformation on the still camera, again the projected grid method was used with equipment listed in Table 6. We had to project the grid with a strobe in order to capture the desired image. Figure 13 depicts the general setup we used in order to capture the glass deformation. In this figure, you can see that the grid is held between the strobe and the subject.

To set up this apparatus, we first moved the apple boxes and BB rifle into place. The grid was placed in the location seen in Figure 13. Next, we moved the 250 W Lowel Pro behind the grid in order to have a constant light source. We used the Lowel Pro to do all of the positioning of the camera and focusing. Before moving the camera into place, we tried to find the location of the grid reflection on our piece of glass. We made any necessary adjustments to the Lowel Pro and the grid.

The Lowel Pro, at this point, is in the location of SPOT in Figure 13. Once we positioned the camera, we focused on the grid projected by the piece of glass. This was important in capturing the glass deformation. Once we were confident that the camera was focused correctly, we replaced the Lowel Pro with SPOT, trying to place in SPOT in the position held by the Lowel Pro. Then, we turned all of the lights off in the room and ran tests to make sure we were getting a good exposure and that SPOT was positioned correctly. The camera was set to "bulb," and we opened the shutter. Then, we manually triggered SPOT to strobe and closed the shutter. We looked at the recorded image of the grid and adjusted the camera aperture and the position of SPOT and repeated this as needed until the exposure looked good.

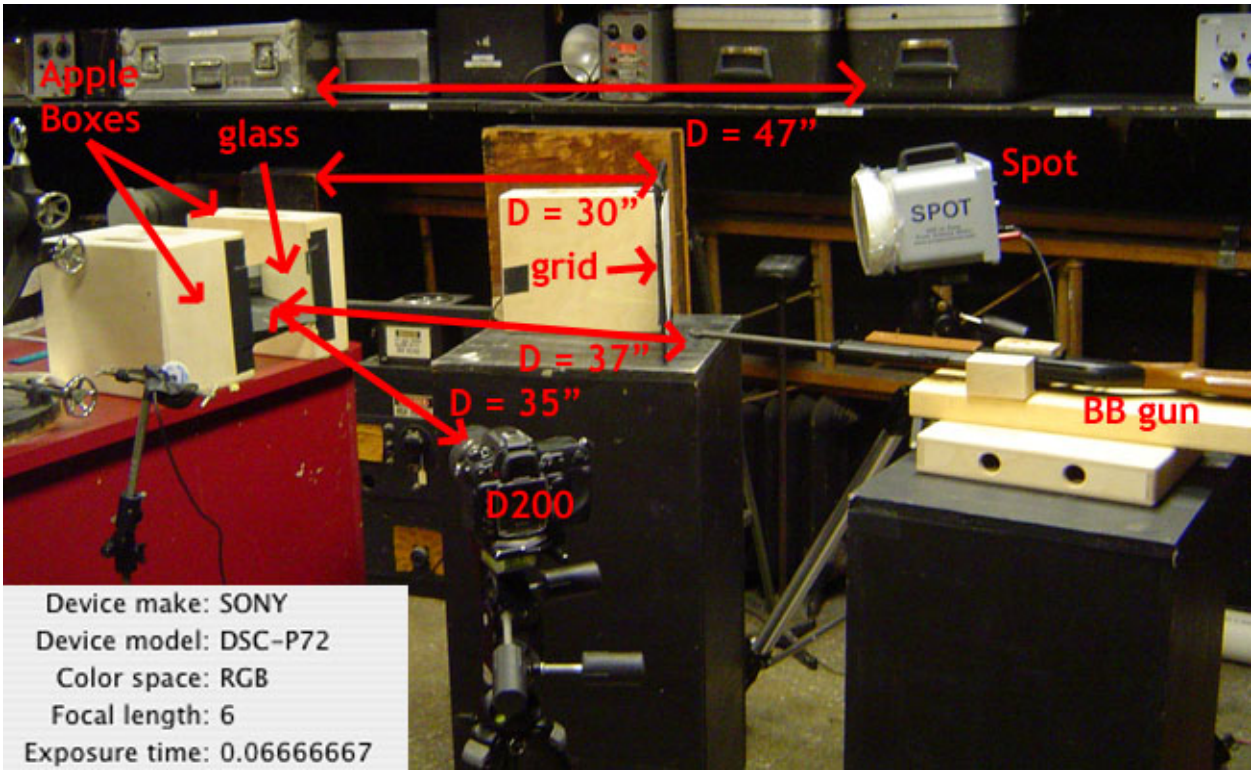

Figure 13: Setup for capturing still images of glass deformation using a projected grid method. The grid is formed from left to right, a piece of chicken wire, a sheet of plexiglass, and a sheet of paper taped together. This creates a grid that also diffuses the light source.

After positioning SPOT, we needed to create a triggering mechanism to make SPOT strobe when the BB impacted the glass. The idea behind this is that a beam from the beam break trigger will be reflected off of the glass into the detector. When the BB impacts the glass, the beam is reflected away from the detector and the trigger is triggered. We set up the beam as in Figure 14. The output of the trigger was put into the Time Machine. The Time Machine was set up with a timeout of 4 seconds and the output of the Time Machine was fed into SPOT. SPOT was set up with no delay.

In order to capture the images, we repeated the following procedure for each sheet of glass:

1. Tape glass to the apple boxes.
2. Confirm the trigger is functioning by tapping the glass and making sure SPOT flashes.
3. Pump the BB gun to the correct pressure, and chamber a BB.
4. Place the gun in the wooden shooting harness (see Figure 13).
5. Aim the gun.

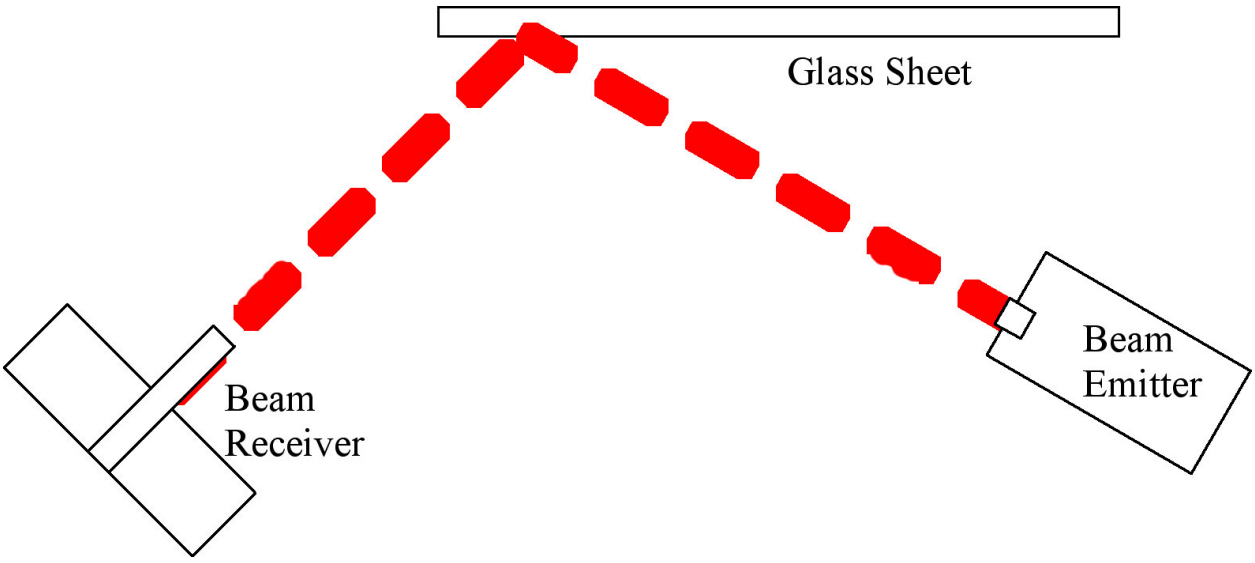

Figure 14: Setup for triggering strobe SPOT. The output of the trigger was put into the Time Machine. The Time Machine was set up with a timeout of 4 seconds and the output of the Time Machine was fed into SPOT.

6. Ensure everyone is wearing safety glasses.
7. Deactivate the gun's safety.
8. Turn off the lights.
9. Open the D200's shutter.
10. The shooter hears the shutter click and fires the gun.
11. The shutter is closed when strobe flashes.
12. Turn lights back on.

We repeated this over several trials.

3.4 Schlieren Imaging

Table 7: Materials for Schlieren imaging experiment.

Item	*Manufacturer*	*Model*	*S/N*
Heat gun	Accupro	1500 Watt	—
Tripod (for Phantom camera)	Manfrotto	3021BPRO	—
Titration device	DNR	DNR	—
Lab Stand, clamps	—	—	—
Water	—	tap water	—
Schlieren Setup	—	—	—
Light source	—	DNR	"1"
Roscolene gels	Rosco	2001,89,70,310	—
NTSC video camera	Sharp	XC-900D	211325
DV camera	Panasonic	PVGS-400	H5HG50513
Digital multimeter	Fluke	179	93810559
Type K thermocouple	Fluke	—	—

For Schlieren experiments, we used the Schlieren setup[1] in lab. The projector is designed to work as shown in Figure 15.

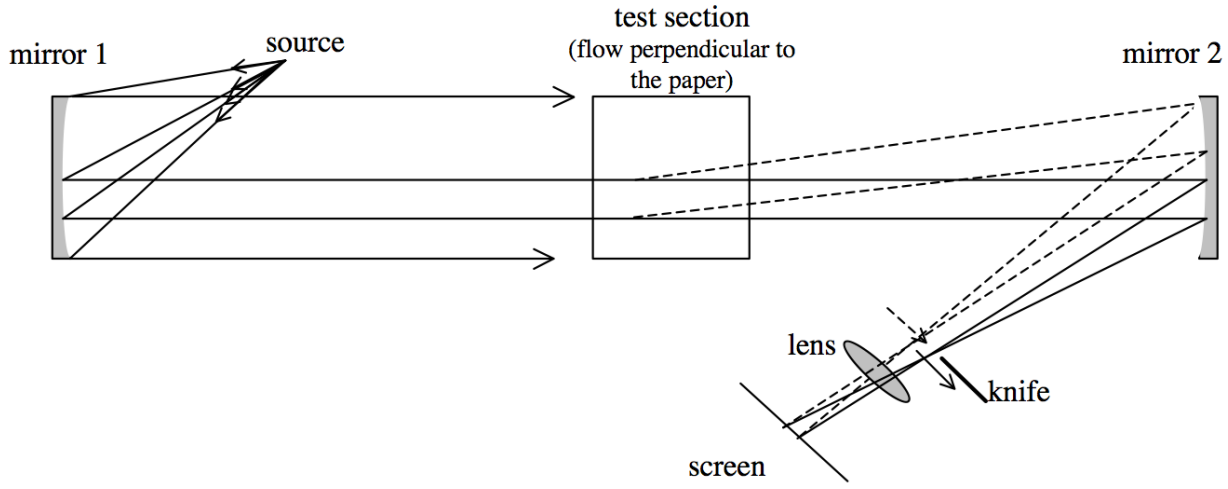

Figure 15: Diagram of a Schlieren Photography System [Jeronimo]

For our experiments, we suspended a piece of glass within the Schlieren field of view with a ring stand clamp. The glass was held from one side. We then heated the glass with the heat gun. Once the temperature of the glass, stopped increasing, we removed the heat gun and dropped a droplet of water from a titration device onto the glass. The specific used materials are listed in Table 7.

[1]the "setup" includes parabolic mirrors, adjustable knife-edges, tabletop, etc.

4 Results

As mentioned under "Procedure," there were a number of pieces to this lab, each with a distinct set of results. To recapitulate, we looked at the impact of thermal shock, at the beam break and optical trigger mechanisms, at means for breaking sheets of different thicknesses, and at different lighting techniques.

4.1 Thermal Shock

For the testing of thermal shock, as described under "Procedure," we determined that neither a heat gun nor a soldering iron alone were sufficient to crack glass.

Heating the glass and then rapidly cooling it with water, however, was able to break glass under certain conditions. The initial height of the water-dropping mechanism, as well as the volume of water dropped, both appeared to be important. This effect can be seen in Figures 16 and 17.

Figure 16: The first of two images showing a crack propagating through glass. HSV settings are shown.

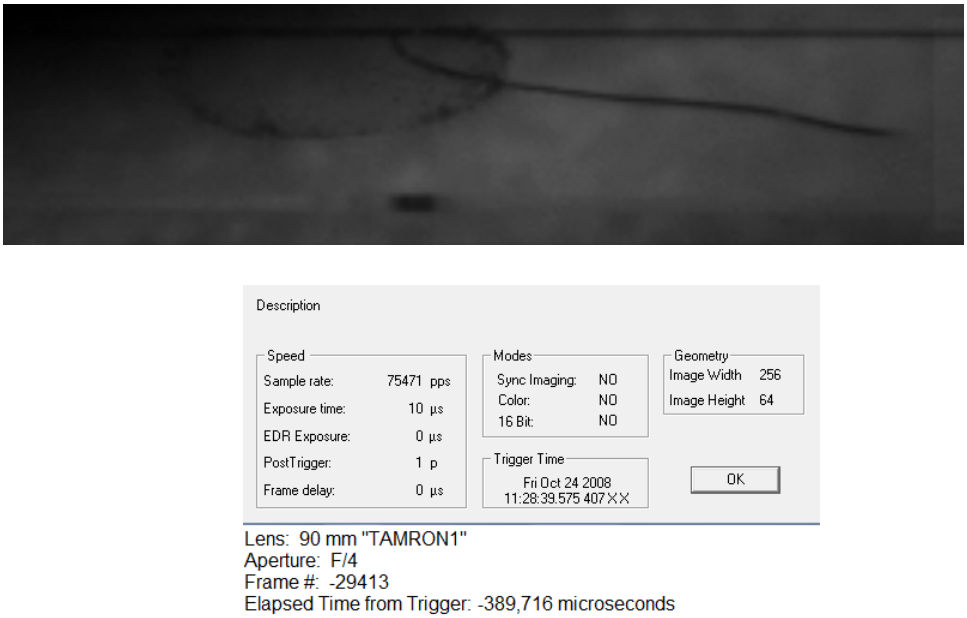

Figure 17: The second of two images showing a crack propagating through glass, taken 93 μseconds after the first frame. HSV settings are shown.

4.1.1 Trigger Mechanisms

We had relatively good results with the beam break trigger but relatively poor results with the optical trigger. The beam break trigger seemed to fire relatively consistently when water was dropped through its beam, though during setup and testing, we did experience droplets that failed to cause a trigger.

The optical trigger, however, frequently failed to trigger at all in the presence of a drop of water. We were not able to gather useful data on it because we were unable to get it to work reliably.

Experimentally, it seems that lighting has a significant impact on the optical trigger. If a light was pointed directly at the trigger's sensor mechanism, it was likely to not trigger at all, whereas it seemed to work when only in the presence of ambient room light. Adjusting the sensitivity of the Time Machine that interfaced with the trigger helped, but did not entirely resolve the problem.

4.1.2 Lighting Techniques

For testing different lighting techniques, the goal was to find the most visually effective form of lighting rather than to calculate any specific data. Towards that goal, we generated images from backlit and side-lit slides, as shown in Figures 18 and 19.

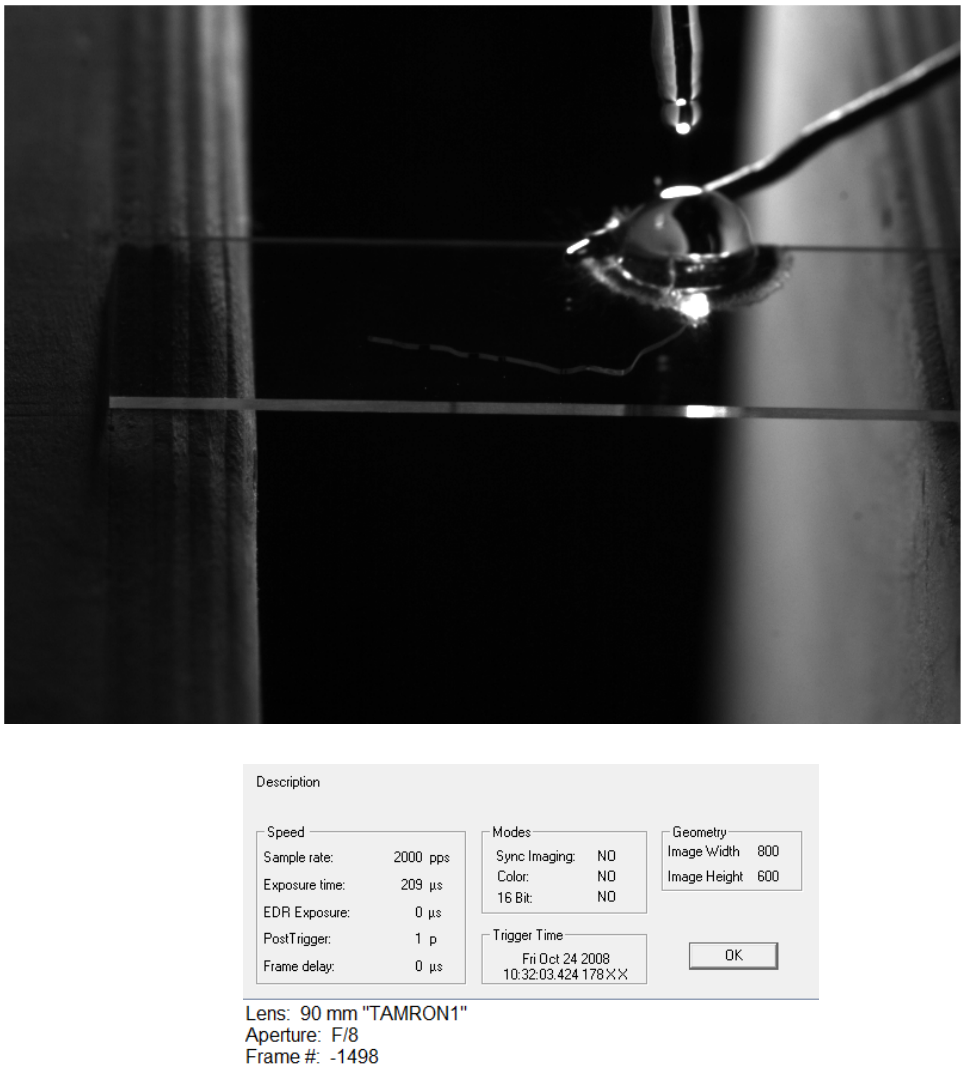

Figure 18: This image was captured with a side-lit microscope slide, lit against a black background. The displayed settings were used.

We found that standard lighting was not particularly effective. Both side- and back- lighting were effective. Shooting a slide from underneath, however, produced images that were surprisingly unclear. We quickly discontinued this strategy as we could not easily tell what was going on in the images that it produced.

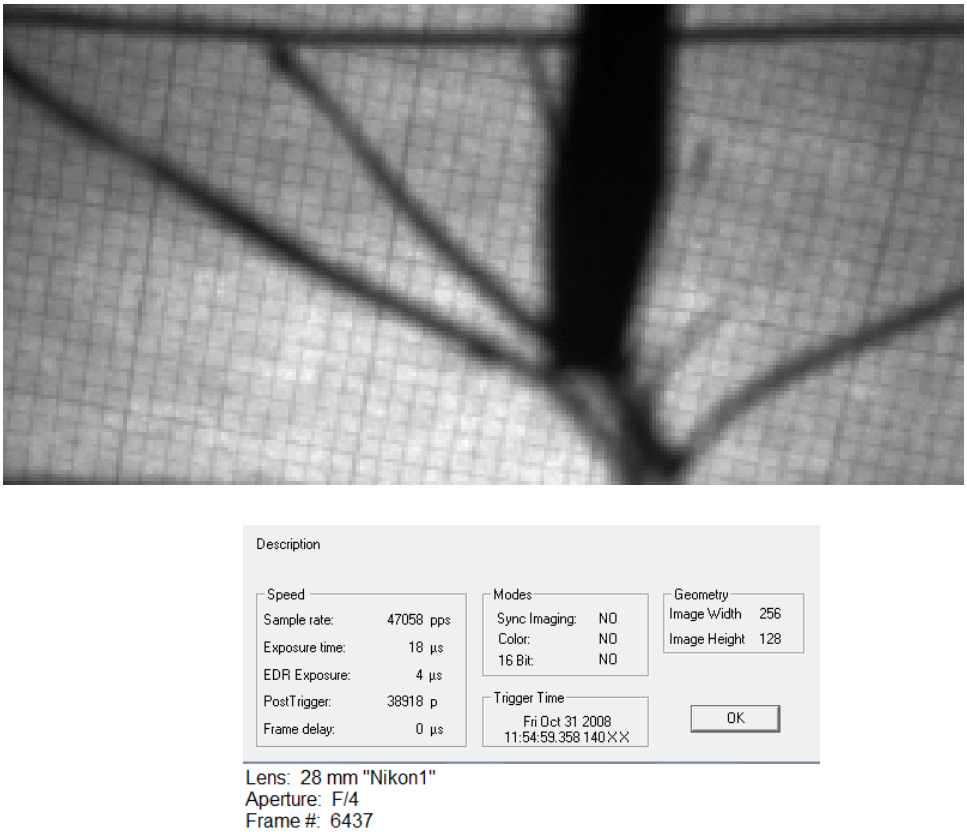

Figure 19: This image was captured with a back-lit microscope slide. The displayed settings were used.

4.2 Mild Impact

We found that the thicker $^3/_{32}''$ sheet glass was much harder to break than the thinner microscope slides. We tried dropping objects from various different heights onto the glass. Based on this data, we gathered the glass-breakage data listed in Table 8.

The pendulum used for these experiments was a piece of PVC pipe roughly $12''$ long and $1''$ in diameter, hinged at the top so that it can swing freely around one axis and with an exposed bolt head on its end facing in the direction of swing. This pendulum was used in a previous lab for popping balloons.

Table 8: Glass Impact Data

Glass	*Implement*	*Height*	*Break?*
Slide	Pendulum	$1''$	Yes
Slide	Screwdriver	$1''$	Yes
$^3/_{32}''$	Pendulum	$1''$	No
$^3/_{32}''$	Pendulum	$3''$	No
$^3/_{32}''$	Pendulum	$12''$	No
$^3/_{32}''$	Screwdriver	$2''$	No
$^3/_{32}''$	Screwdriver	$4''$	No
$^3/_{32}''$	Screwdriver	$8''$	Yes
$^3/_{32}''$	Screwdriver	$12'$	Yes

While our control experiment was able to break $^3/_{32}''$ glass at a height of $8''$ with a screwdriver, later tests were unable to do so consistently.

4.2.1 Glass Flexing on Impact

We intend to see if the glass flexes when impacted with a blunt object. In order to analyze this we will use the below two frames. One right before impact and one right after impact (Figure 20).

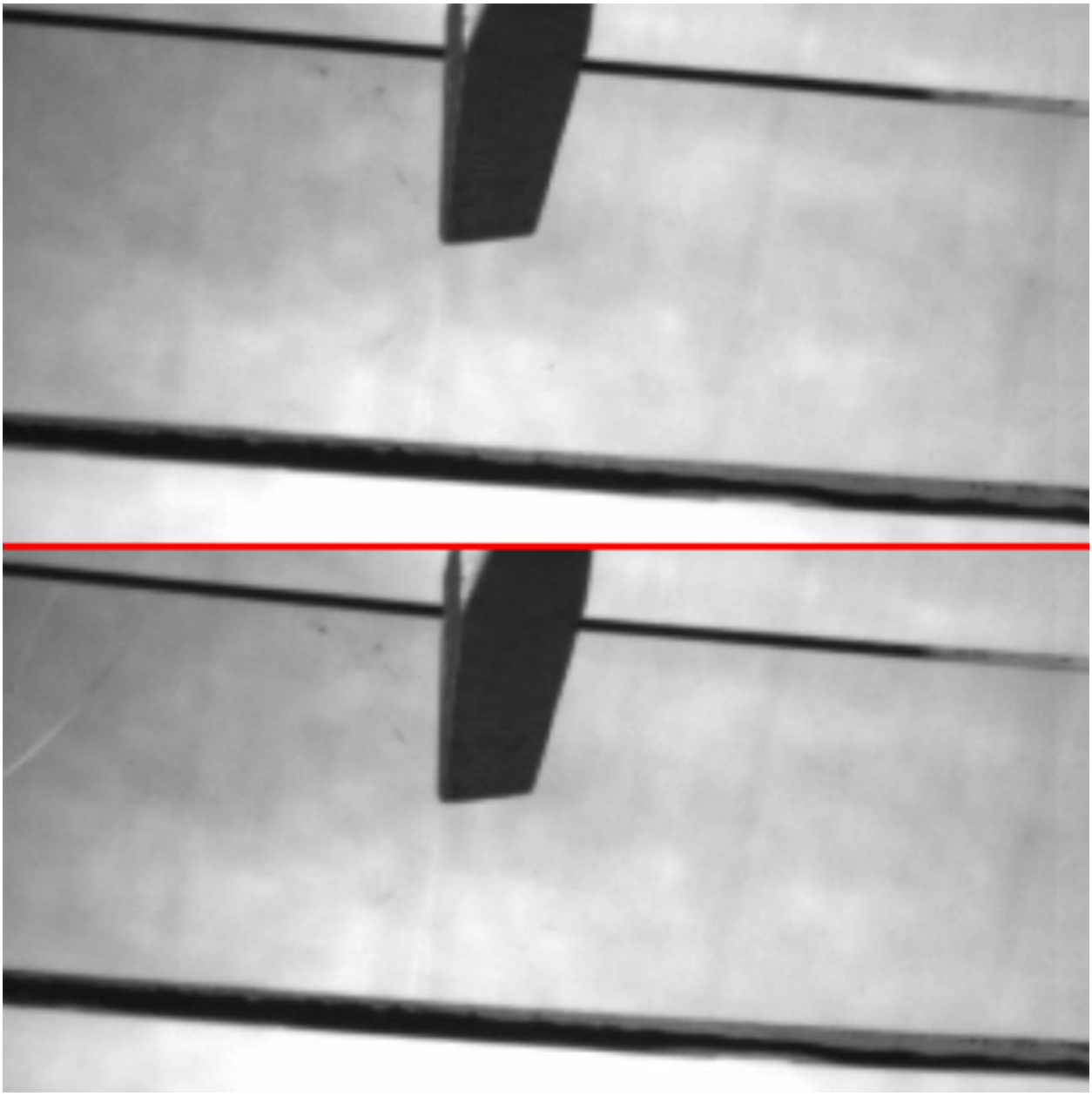

Figure 20: Two consecutive frames of the glass being broken by the impact of a screwdriver. Phantom camera. 28 mm lens. Frame rate 47,000 fps. $8 \times 2 \times {}^{3}/_{32}''$ glass sheet.

4.3 BB Rifle Fired at Glass Slides and Sheets

4.3.1 Crack Formation

We did several trials to see the crack formation as a BB impacts glass. Figures 21 and 22 are a set of ten consecutive frames that show how cracks form when a BB impacts glass.

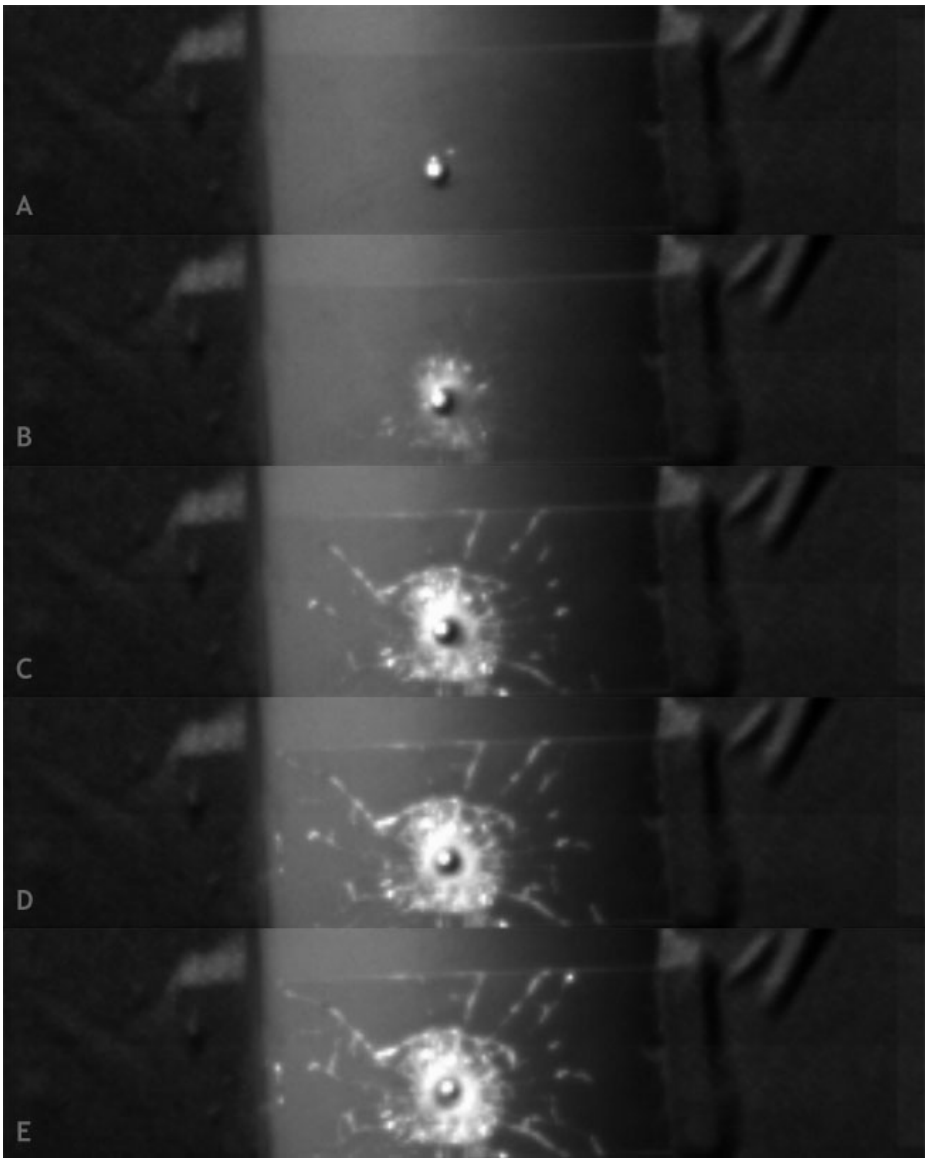

Figure 21: Parts A through E. The first five frames of a BB impacting a glass slide. Phantom camera with aperture f/1.8 and 50 mm lens. 75,000 fps.

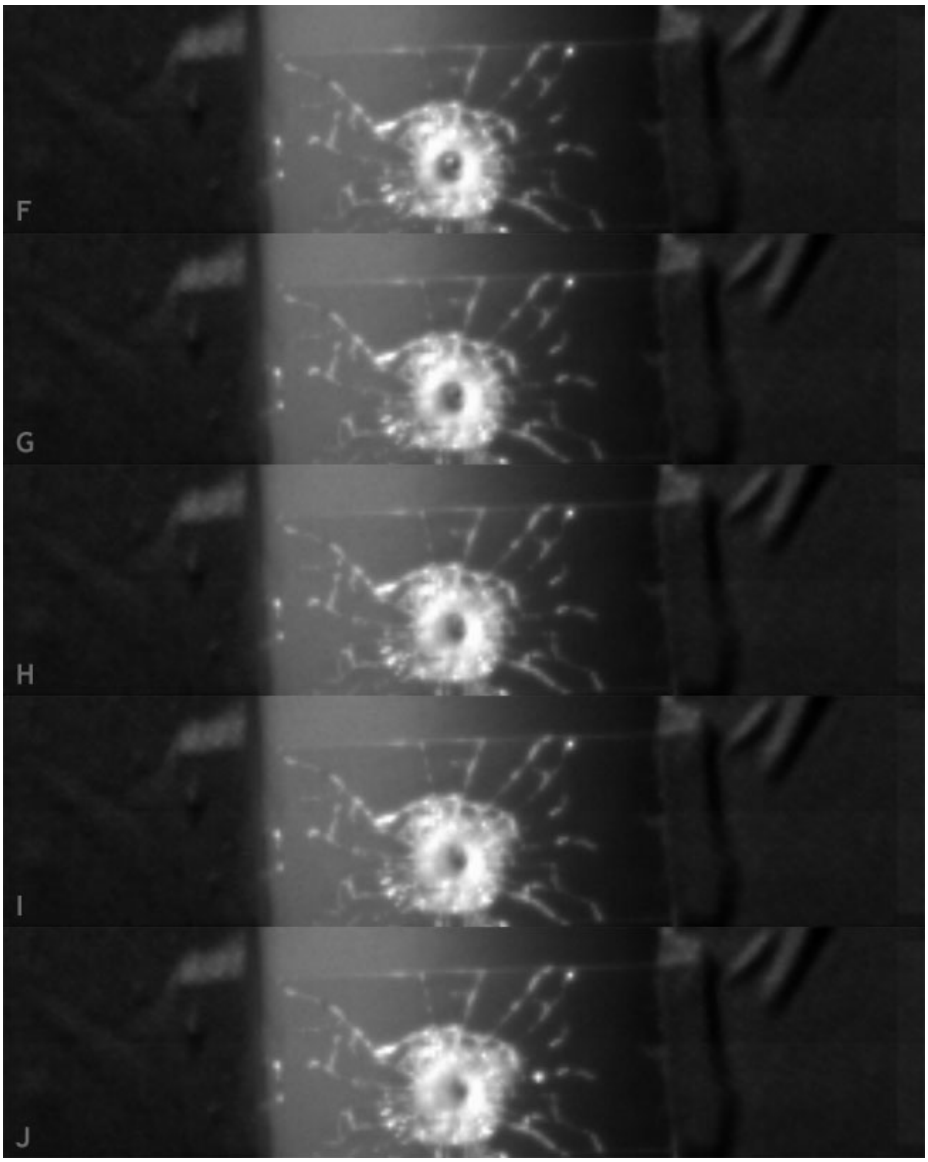

Figure 22: Parts F through J. The second five frames of a BB impacting a glass slide. Phantom camera with aperture f/1.8 and 50 mm lens. 75,000 fps.

4.3.2 Deformation with HSV — Our First Try

In our first attempt to do the projected grid method described in the background, we obtained the following results. Figure 23 is five consecutive frames of a BB impacting glass, captured using the grid reflection method.

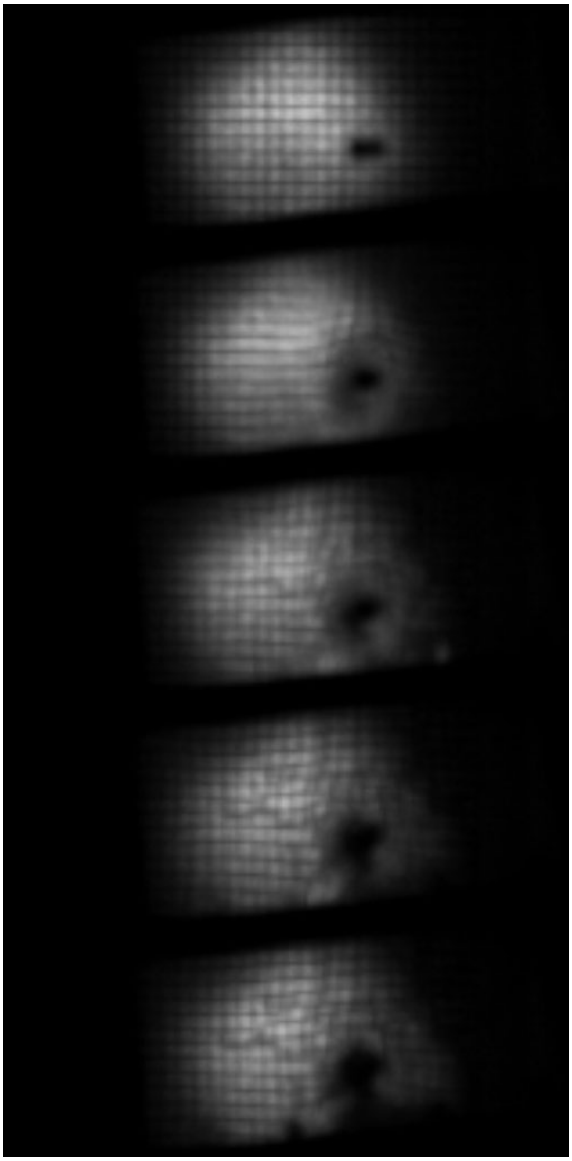

Figure 23: Five consecutive frames of BB impacting glass with projected grid. This glass piece was $8 \times 1\frac{1}{8} \times \frac{3}{32}''$. The Phantom camera was used with f/2.8 and 75,000 fps. 4 pumps on the BB gun. 28 mm lens. Exposure time 18.25 μseconds.

4.3.3 Deformation with HSV — Our Second Try

We ran several trial runs of this experiment. A number of trials were run with mirrors. However, in many of these trials the mirrors did not shatter. It was found that the silver reflective mirror surface held the cracked glass together, preventing it from shattering.

We present 2 trials of grid deformation with this setup.

In one trial with the $3/32''$ glass, we obtained the two images shown in Figure 24. The two consecutive frames shown in this figure illustrate the glass deforming substantially on impact with the BB. This deformation can be seen more clearly in the charts shown in Figure 25. These charts show plots of the positions of the vertices of the wire mesh that are visible in the image.

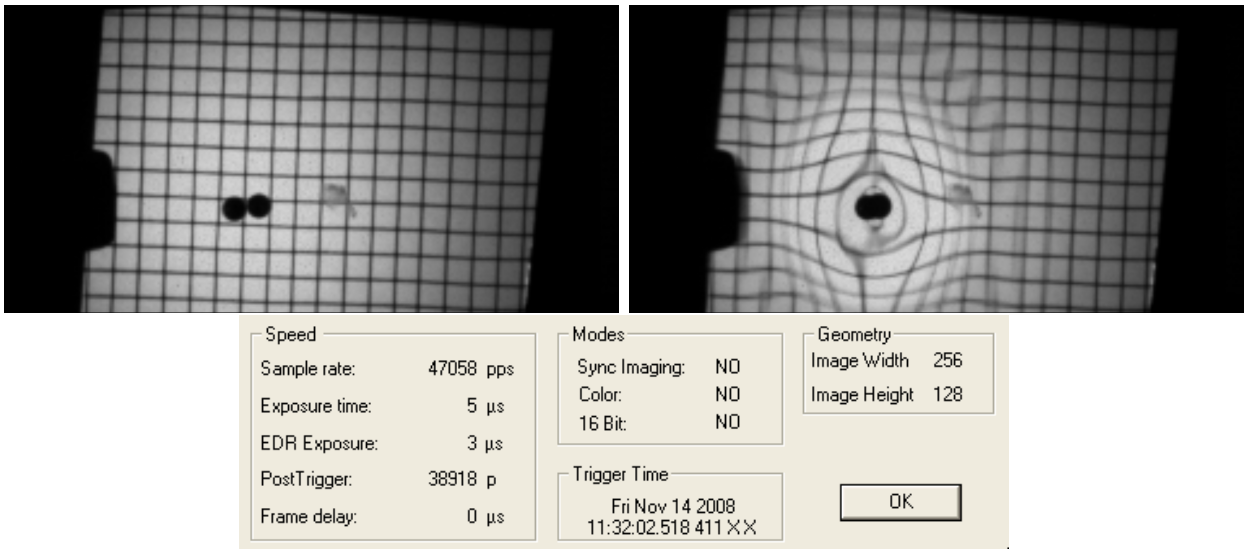

Figure 24: Two consecutive frames of the "projected grid" method from Trial 1. The first frame is immediately prior to the BB's impact; the subsequent frame is immediately after the BB's impact.

The glass deformed in a circular region surrounding the impact point of the BB. The amount of deformation decreased with distance from the BB, up to a certain radius at which the magnitude of the deformation rapidly dropped to zero.

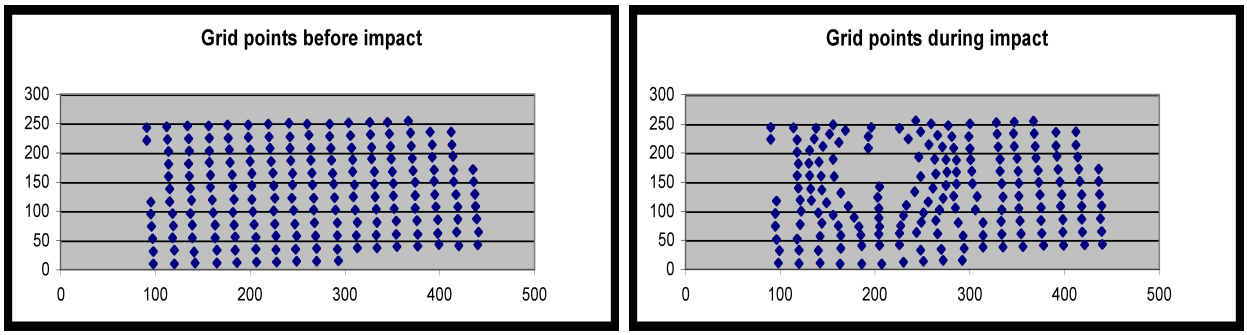

Figure 25: Graphs of the grid vertices from Trial 1, as shown in Figure 24. Units are in "image pixels." The image that we worked with was scaled up to a resolution of 512×256 prior to gathering the data for these charts.

In a subsequent trial with the $3/32''$ glass, we obtained the series of images shown in Figure 26. The images show a similar deformation. The third image in the series exhibits a number of irregular deformations; it appears that, in this frame, the glass has begun to crack. Interestingly, these odd deformations do not show up effectively in the vertex graphs in Figure 27. The cracks manifest themselves as disjoint lines, which are very visible to the naked eye but which don't necessarily have a large or consistent effect on the positions of grid vertices.

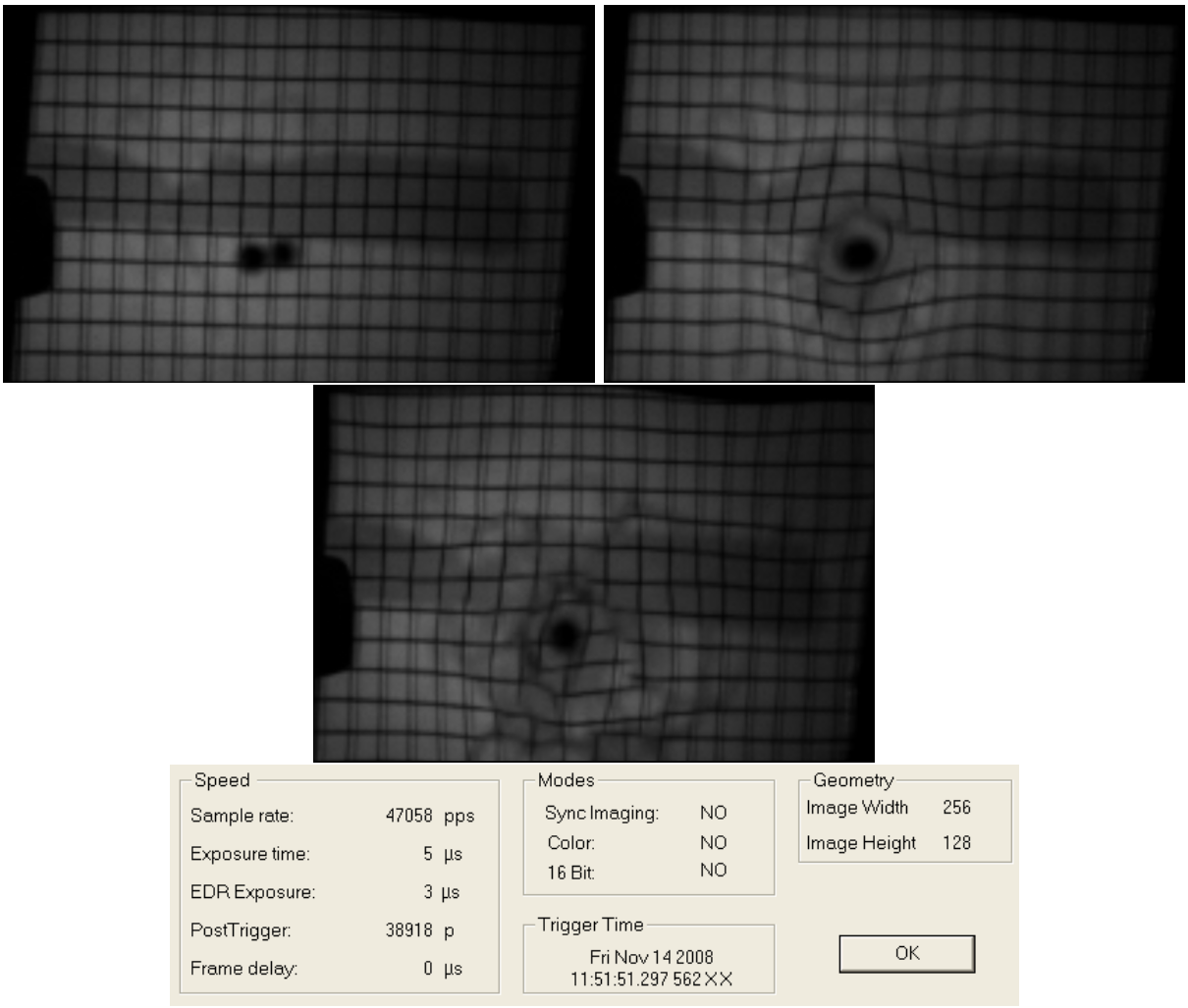

Figure 26: Three consecutive frames of the "projected grid" method from Trial 2. The first frame is immediately prior to the BB's impact; the second frame is immediately after the BB's impact, and the third frame shows the glass beginning to crack.

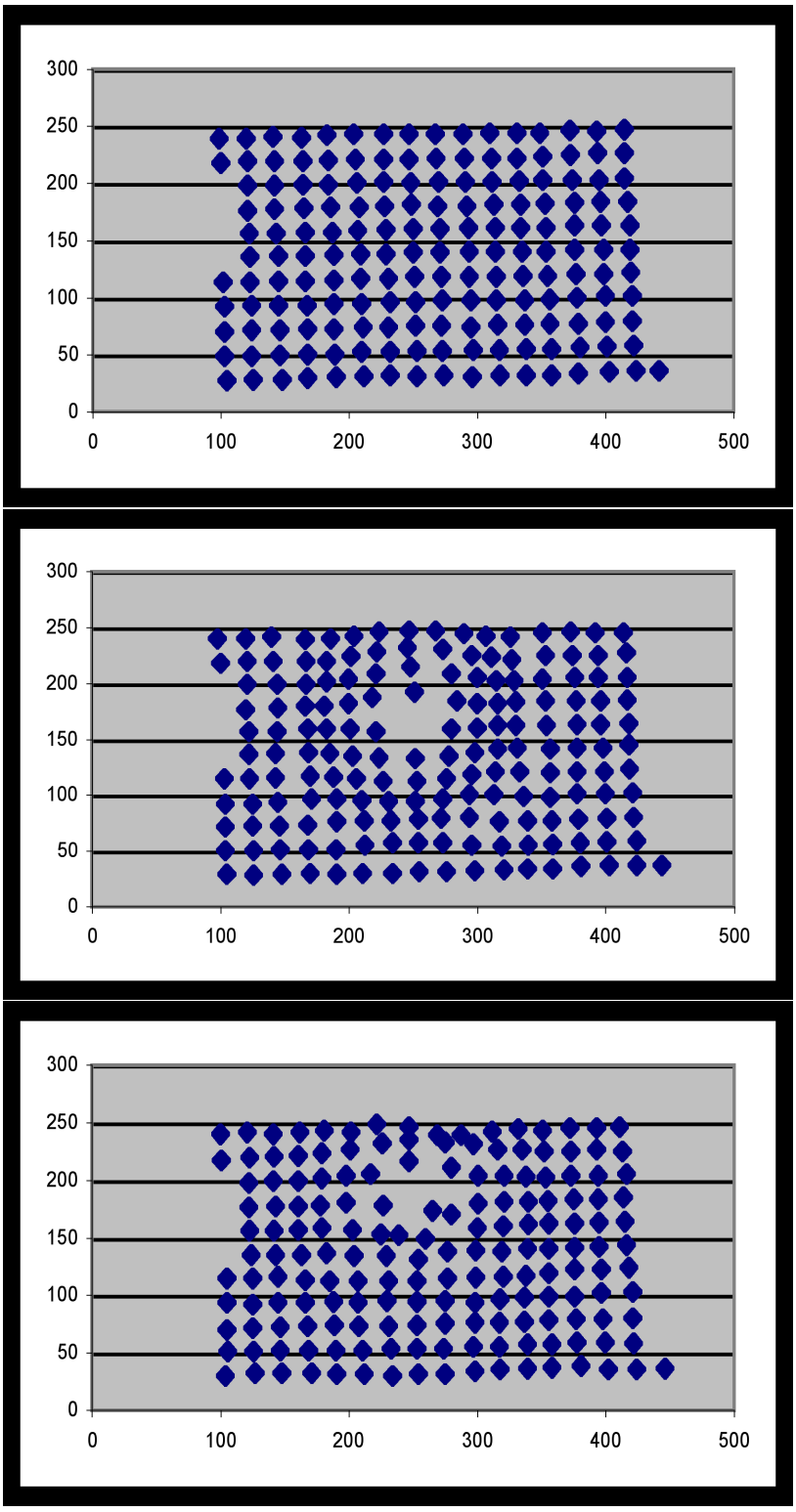

Figure 27: Graphs of the grid vertices from Trial 1, as shown in Figure 26. The image that we worked with was scaled up to a resolution of 512×256 prior to gathering the data for these charts.

4.3.4 Deformation with Still Images

Figure 28 is a still image obtained using sync-and-delay and the Nikon D200 camera. The photo depicts a BB hitting a glass sheet. that is $8 \times 2 \times {}^{3}/_{32}''$.

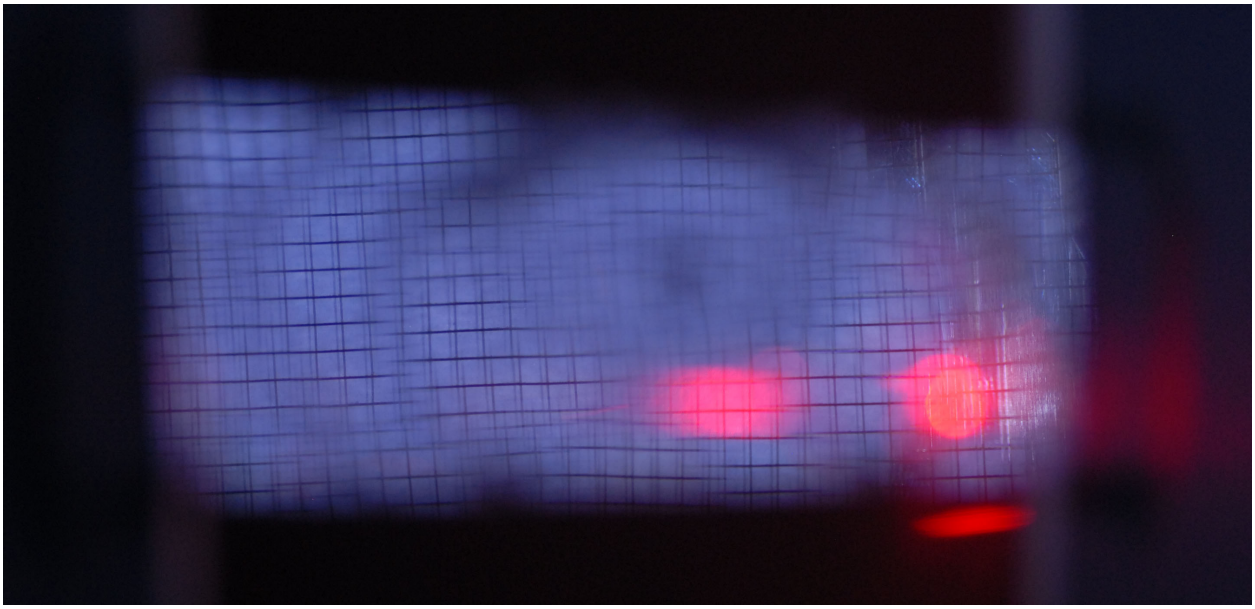

Figure 28: Still image of glass deformation using D200 camera. Camera aperture f/3. Shutter speed set to "bulb." 4 pumps on the BB gun. No added delay in the system.

4.4 Schlieren Imaging

Our Schlieren imagery did not provide frames showing the deformation of glass. We were able to acquire relatively few good video images of glass cracking. Figure 29 shows our best captured recording of glass cracking.

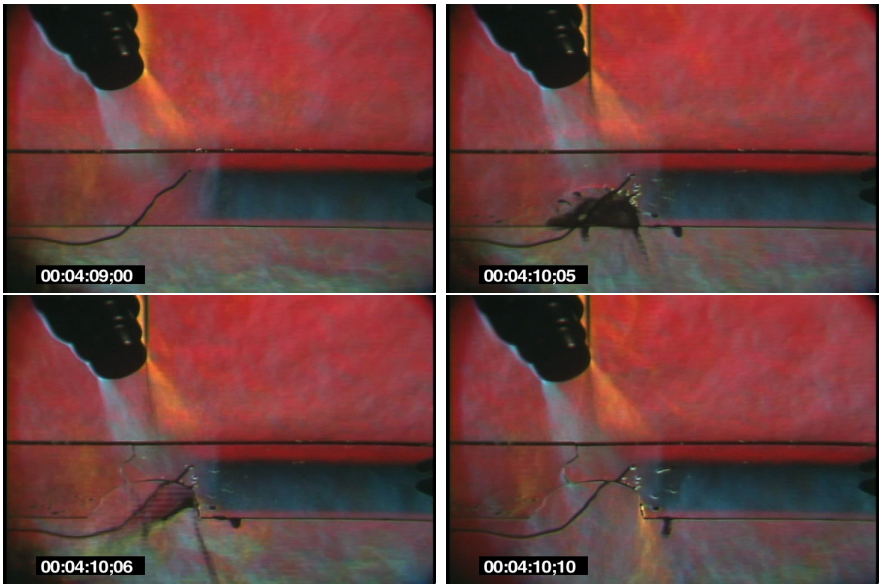

Figure 29: Frames from a captured Schlieren video of glass cracking under heat shock. The video was taken at 30 fps with an NTSC camera; a frame counter is included in the bottom left corner of the frames.

5 Discussion

5.1 Thermal Shock

We found that, while we do not yet fully understand how thermal shock causes glass to crack and shatter, we are able to shatter it consistently.

As mentioned in "Results," the inconsistency of the optical trigger seemed to be correlated with ambient light. We suspect that the sensor was flooded with too much light. It might work better in a darker room (though such a setup would not work for HSV recording). Because the sensor is infrared-based, and because the HSV camera is monochromatic and sensitive to an array of different light frequencies, we might also be able to run the experiment with a strong monochromatic visible-spectrum light. We could also use a still camera in a dark room with a flash. However, since the beam break trigger works most of the time, we decided to use that trigger.

We found both the back-lighting and side-lighting techniques to be effective. They tend to produce inverted images: white-on-black vs. black-on-white. We do not have an immediate use for this fact, but it may well prove useful in future analysis and so is worth keeping in mind.

Based on the high-speed video that we captured and on the images shown in Figures 16 and 17, we calculated a crack propagation rate of 430 m/s in microscope slides.

5.2 Mild Impact

5.2.1 Glass Flexing on Impact

Glass is a hard material, however it is known to flex before breaking. We wanted to test this assertion as well as see if we could capture this flexing. In order to analyze this, we will use the images presented in Figure 20 in the Results section. To see the change in motion of the glass from one frame to another, we will overlay the two images and measure in pixels the change in displacement. Figure 30 shows the two frames side by side. The images are placed next to each other where the screwdriver impacts the glass, which is the point that will flex the most. The left side is the first frame. The right side is the second frame. Red lines are placed to show where the glass from the non-flexed frame would extend if the glass had not been contacted by the screwdriver.

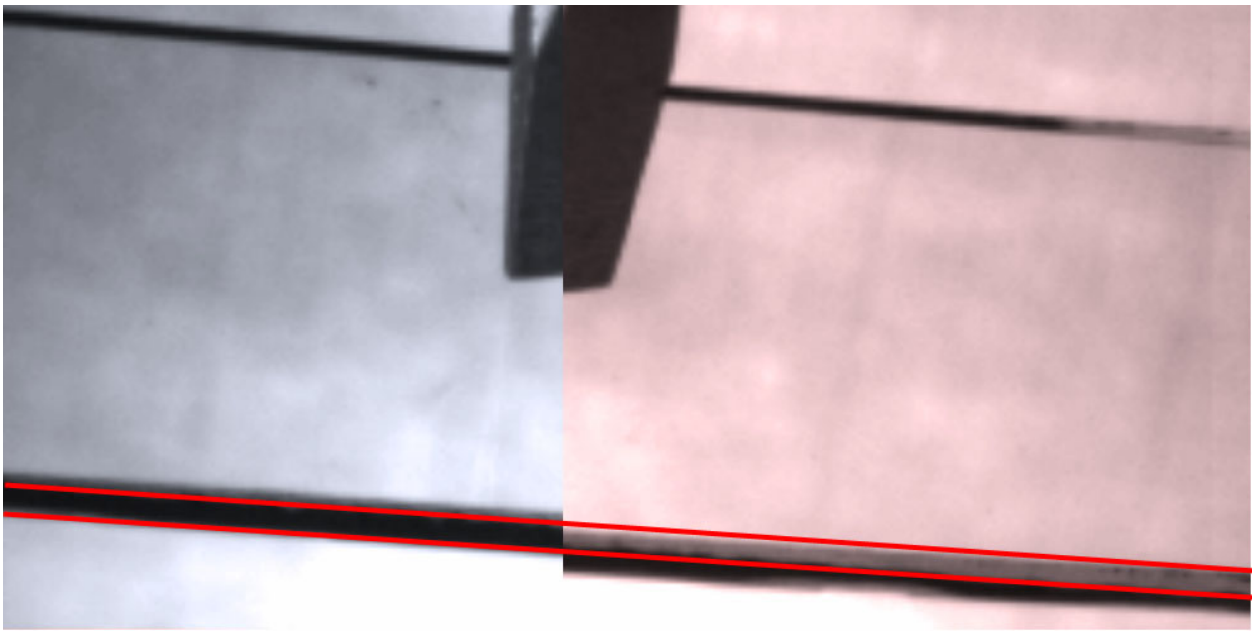

Figure 30: Overlay of two consecutive frames from Figure 20. Phantom camera with 28 mm lens. 47,000 fps. $8 \times 2 \times {}^{3}/_{32}''$ glass sheet. The left is the first image and the right is the subsequent frame. The red lines extend the edge of the non-flexed glass to show visually how the glass has flexed.

To analyze this, the image is calibrated using the known thickness of the glass of ${}^{3}/_{32}''$, which is $0.094''$. We measured the thickness of the glass in the screenshot at 23 pixels.

$$\frac{\frac{3}{32}}{23} \Rightarrow \frac{3}{736} \text{ inches/pixel}$$

The image displaces by 15 pixels. Changing this back to inches gives us $0.061''$, or roughly the thickness of the glass.

One problem with light-based triggers in this experiment is that drops of water are clear. They act as lenses, distorting light passing through them; but they do not block light. We hypothesized that using a darker-colored fluid (such as water containing a great deal of food coloring) might lead to better results with both trigger mechanisms.

We established that glass that is 2.4 times as thick requires an impact with much more than 2.4 times the energy in order to shatter. This is not terribly surprising. Mechanics [2.001] teaches us that the resistive moment M is

$$M = \int_A \rho \cdot y dA = \rho \frac{h}{2}^2 \cdot w \tag{4}$$

This means that the strength of the glass varies with both its width and with the square of its thickness. Dividing these two, we get that

$$\frac{(h_1)^2 \cdot w}{(h_2)^2 \cdot w} \tag{5}$$

is the ratio of the moments. Calculating the ratio between a $75 \times 25 \times 1$ mm slide and a $203 \times 51 \times 2.4$ mm pane of glass, and assuming that the two different panels of glass are made from the same glass compounds so that their ρ constants are the same, we get

$$\frac{(2.4)^2 \cdot 51}{(1)^2 \cdot 25} = 12 \tag{6}$$

which would predict that the thicker glass can withstand 12 times the moment of the thinner slide. Our experiments were not targeted at calculating this moment; nonetheless, comparing our data from thin slides to our data from much-harder-to-break $^3/_{32}''$ glass, our results do seem to support this calculation.

5.3 BB Rifle Fired at Glass Slides and Sheets

5.3.1 Crack Formation

From Figure 21 in the results we can see the progression of what happens to a glass slide when a BB hits it. It is apparent in Figure 22, parts F through J that the BB goes through the piece of glass. We can look at this glass and characterize the types of cracks that form. In Figure 31, we can see that there are radial or concentric cracks that form.

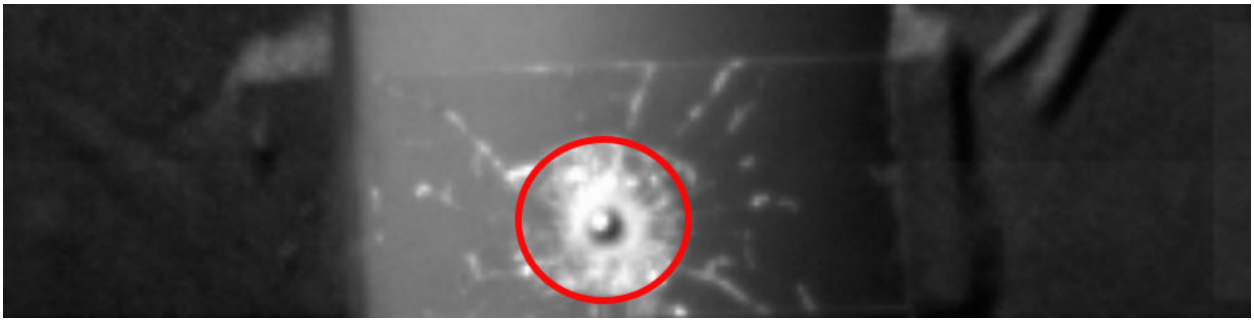

Figure 31: This image extracted from Figure 21, part D. Here, we overlay a circle showing the concentric cracks that form.

In Figure 32, we can see that radial cracks also form.

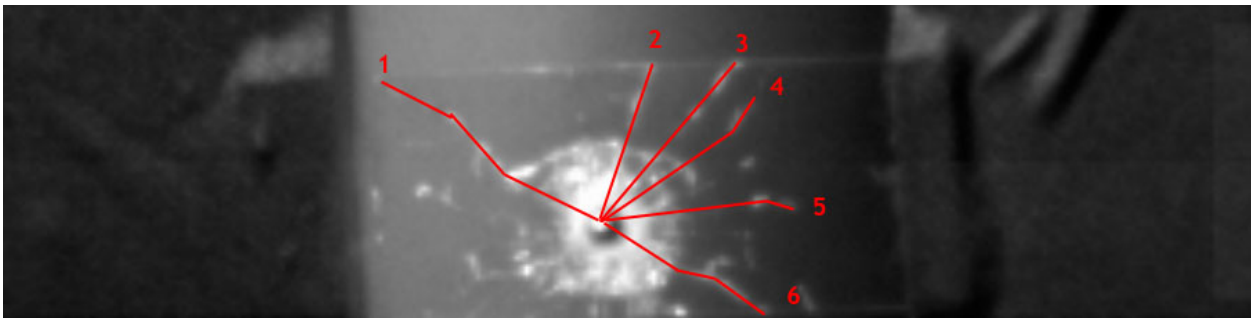

Figure 32: This image is extracted from Figure 21, part D. Here, we overlay lines to show the major radial cracks that have formed. The cracks are labeled 1 through 6.

By looking at Figure 21, parts B through D, we can trace the crack formation over time and calculate the average crack speed. In Figure 33, we placed blue dots at the end of each crack in the first of the three frames, a green dot at the end of the crack in the second frame, and a yellow dot at the end of the crack in the third frame. Then we overlaid the cracks from Figure 32 and the dots indicating crack endings to see the progression of the slide breaking.

Using the image at the bottom of Figure 33, we can measure the distance the crack has moved in pixels. Table 9 illustrates the results obtained by finding the pixel distances.

We can also measure the apparent slide width in the image. It is 178 pixels wide. This

Table 9: Distances traveled by cracks in pixels
(pixels from BB impact)

Crack #	*Blue dot*	*Green dot*	*Yellow dot*
1	—	133	189
2	30	118	—
3	34	143	—
4	—	121	136
5	37	113	142
6	—	129	—

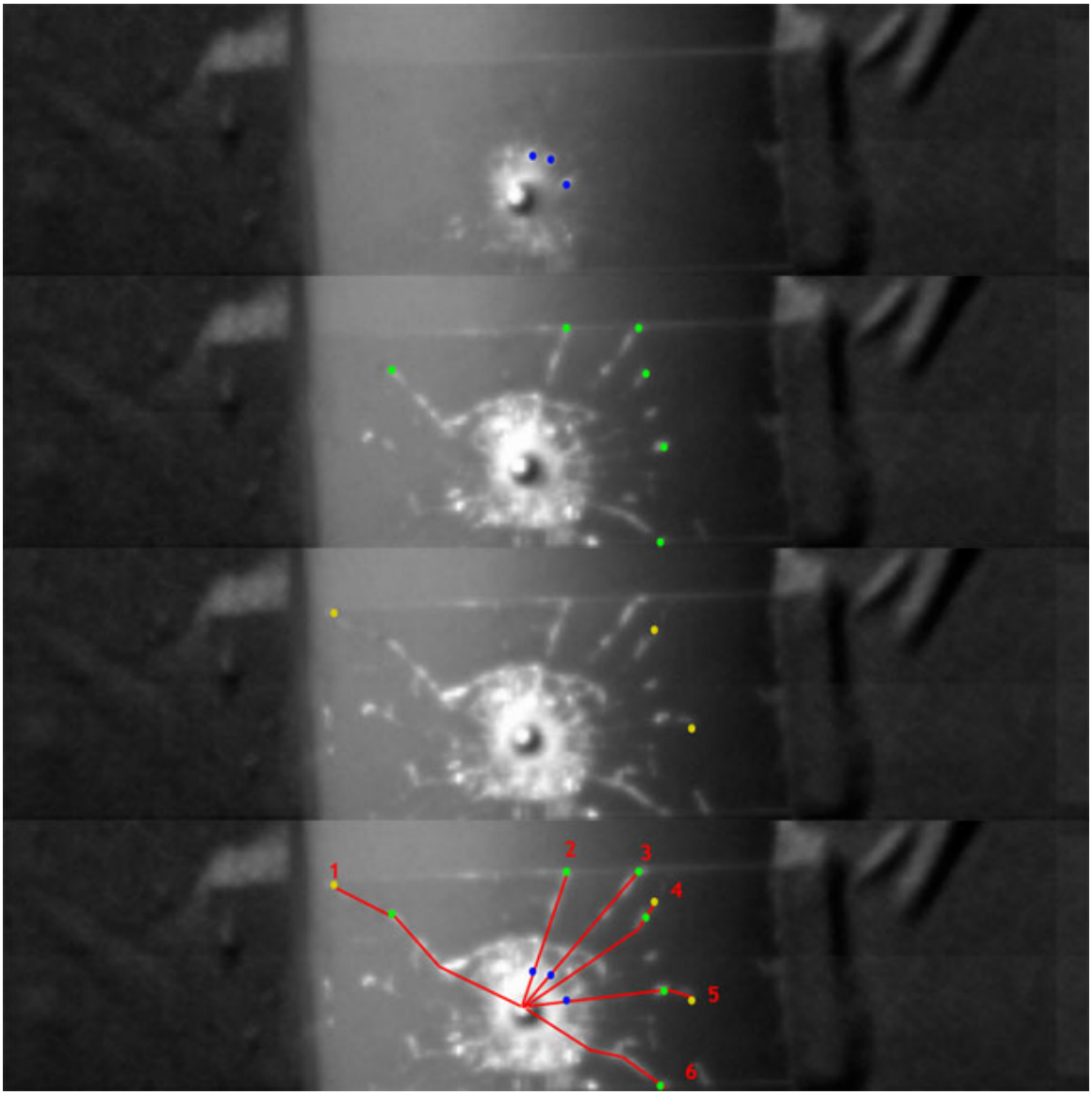

Figure 33: This is using the frames from Figure 21, parts B through D. Here we have traced the crack formation, placing dots at the ends of cracks at this particular stage in the breaking process.

allows us to calibrate the image so that we can find actual displacements. Using the actual slide width of 25 mm, we can see that the we have a ratio of 25 mm per 78 pixels which is 0.32 mm/pixel. Using this ratio, we can make Table 10 with the actual displacements from the pixel displacements.

Table 10: Distances traveled by cracks
(millimeters from BB impact)

Crack #	*Blue dot*	*Green dot*	*Yellow dot*
1	—	43	61
2	9.6	38	—
3	11	46	—
4	—	39	44
5	12	36	45
6	—	41	—

Using the data in Table 10, we can calculate the change in distance from the point of impact of the BB. We can use this information to calculate velocities. Table 11 has the changes in distances.

Table 11: Change in distance from BB impact (in mm)

Crack #	*Blue dot to Green dot*	*Green dot to Yellow dot*
1	43	18
2	28	0
3	35	0
4	39	5
5	24	9
6	41	0

From Figure 33, we can see that only crack 5 expands in all frames. It is important to note that, for all other cracks besides crack 5, we cannot be certain that the crack has been forming for the entire duration between each frame. For example, if we look at crack 1, we see that the crack did not start to form and therefore has no blue dot in Figure 33. This same logic holds for cracks that do not have a yellow dot in Figure 33. We do not know when the crack stopped moving, so the crack may have reached the location of the green dot before the Phantom captured that image for the second frame in Figure 33. For this reason, the time between frames represents the maximum time taken for a crack to travel a specified distance. Thus, the velocity calculations in Table 12 are a lower bound. In order to make the calculations in Table 12, we multiply by 75,000 fps, the frame rate of this sample.

Table 12: Velocities from one point to another (m/s)

Crack #	*Blue dot to Green dot*	*Green dot to Yellow dot*
1	3200	1350
2	2100	0
3	2600	0
4	2900	380
5	1800	680
6	3000	0

Using Table 12, we can see the average velocities of the crack formation for different cracks at different times. As stated earlier, we must use logic to figure out which values are valid. Cracks 2, 3, and 6 do not have yellow dots so the crack stopped moving before the green dot or before the second frame in Figure 33 was analyzed. Looking back at Figure 21, we can see that after part D, the cracks appear to stop forming. This suggests that the cracks stopped well before the frame part D was taken by the Phantom camera. For this reason the velocities found that represent cracks forming between the blue and yellow dots should be the valid values. The range that we have found from this data for the velocity of crack formation is 1800 to 3200 m/s with an average of 2600 m/s.

5.3.2 Deformation with HSV — Our First Try

Figure 23 (§4.3.2) is extremely blurry. We can see that there is deformation in the glass, but beyond that there is not much analysis that we can do. The grid lines are blurred to the point where they are hard to distinguish. The reason for the blurring is motion blur caused by too long of an exposure time. For this reason, in future grid trials discussed later in this report, we increases the amount of light and decreased the exposure time. This information is presented to illustrate how important the short exposure times were and that we learned through trial and error that they were necessary.

5.3.3 Deformation with HSV — Our Second Try

Looking at this data, we were unable to make many generalized conclusions. Based on the data from the grid-vertex location graphs, we calculated the distance that each vertex moved between its rest and deformed positions, and graphed this distance against the vertex's initial distance from the point of impact of the BB. Not surprisingly, we found that pixels closer to the impact site had a strong tendency to move a greater distance within the first few μseconds of the impact. This effect is illustrated nicely in Figure 34, which shows two nodes, one at around 80 pixels (1.3″ from impact) and one at around 140 pixels (2.8″ from impact). The first node appears to be the expected edge of the deformation as the bullet pushes the glass inwards. We are not certain what causes the second node.

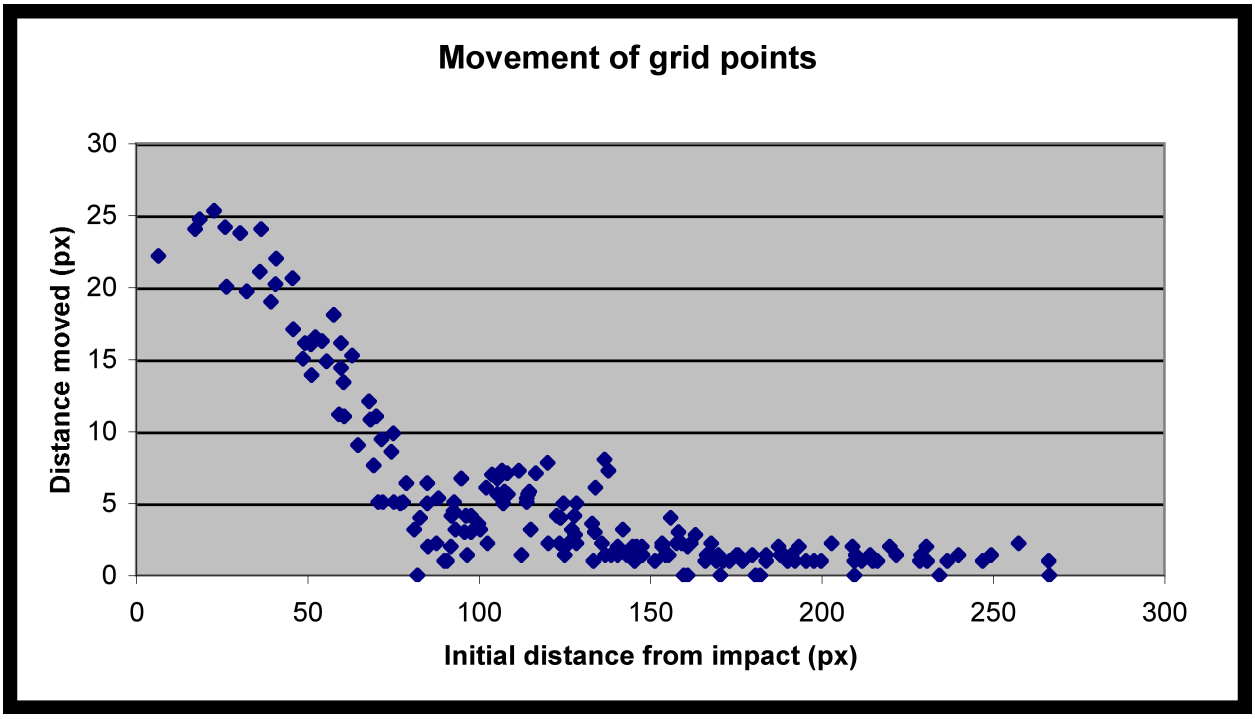

Figure 34: Graph of Point Displacement vs. Point Radius. 50 pixels = 1″.

With our two-frame trial run, we were able to compare two consecutive sets of position changes. As can be seen in Figure 34, in the first 13 μs after the impact of the BB, the glass deforms as in the first trial; but in the second 13 μs, the glass near the BB doesn't show much deformation (probably because it has begun to crack), but there is a ring of deformation at a radius of around 100 pixels (2″ from impact). We do not know if this is caused by a shock wave propagating outwards at some velocity or by a secondary local deformation caused by the cracking of the glass.

If we make the assumption that the second peak in the second chart is caused by a shock wave propagating outwards, we can attempt to estimate that shock wave's velocity. In Figure 35, we examine the radial distances of the pixels that moved the greatest distance within the

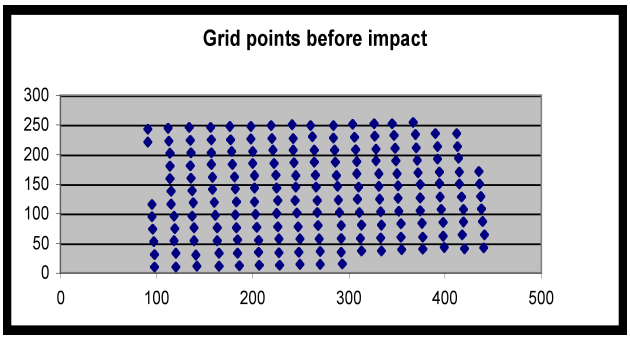

Figure 35: Graphs of the grid vertices from Trial 1, as shown in Figure 24

specified time windows, and take their distance from the impact site to be the radius of the shock wave. Making this assumption, we have two radii (measured at 23 and 87 pixels, respectively), and a time delta (13 μs). This gives us a velocity of 1,530 m/s.

As noted in Table 13, waves propagate at speeds that are on the same order as 1,530 m/s. The slowest propagation rate is roughly 1.5 times the number that we calculated for a possible propagation velocity. This is far enough off that it is unlikely that what we are seeing is strict wave propagation, but it is close enough that what we are seeing is likely a related phenomenon.

Table 13: Speed of sound in glass

Glass Type	*velocity of longitudinal waves (m/s)*	*velocity of shear waves (m/s)*
Fused Silica	5968	3764
Glass, heavy silicate flint	3980	2380
Glass, light borate crown	3980	2380
Glass, pyrex	5640	3280

Sources of Error There are a number of possible sources of error in this data. One error source is the resolution, both pixel resolution and time resolution, of the Phantom HSV camera. Capturing video of an event as quick as the deformation that we are interested in is at the edge of the Phantom's range. We had to use a frame rate near its maximum, and as a result an image resolution near its minimum, to get any deformation imagery at all. This has two effects: first, we are only able to view at most two frames of deformation prior to cracking, so we have very few frames and relatively little timing data to work with. Second, there are only about 10 pixels between each vertex in the grid that we are watching, so an error of a single pixel has a substantial impact.

Additionally, the software that we used to find the pixel locations of the grid points was quite simplistic, and depended on a lot of human interaction. It was easy for a point measurement to be off by one or two pixels.

Based on these factors, we expect the position error to be on the order of ± 2 pixels, or $1/12''$.

We are interested in time estimates on the order of two or three frames, so time error may be as much as half a frame duration, or 7 μs.

We feel that the experiments that we ran were approximately as thorough as possible given the limitations of the Phantom HSV camera. Were we to repeat the experiments, we would follow the same procedure. However, there would be substantial benefit to a future group with more sophisticated analysis software and an HSV camera capable of higher frame rates at a higher resolution, re-running these experiments to attempt to gain data with greater accuracy.

5.3.4 Deformation with Still Images

Looking at Figure 28 (found in the Results), the image appears to be blurry. We are unsure what caused this to occur. Some of our hypotheses include:

- the duration of SPOT's flash creating too long of an exposure to image the speeds of the shock waves without blur
- the aperture of the lens being large enough that the deformed glass was out of the depth-of-field of the camera

It was difficult to confirm if either or both of these were factors leading to this phenomenon.

We do learn some things from this D200 still image. In Figure 36, which is copied from Figure 28, we have drawn an "x" to indicate where the BB impacts. Around this "x," we can see circular waves emanating out from this location as one might see in water if a rock is thrown into the water. This phenomenon is consistent with what we saw with the high-speed video camera.

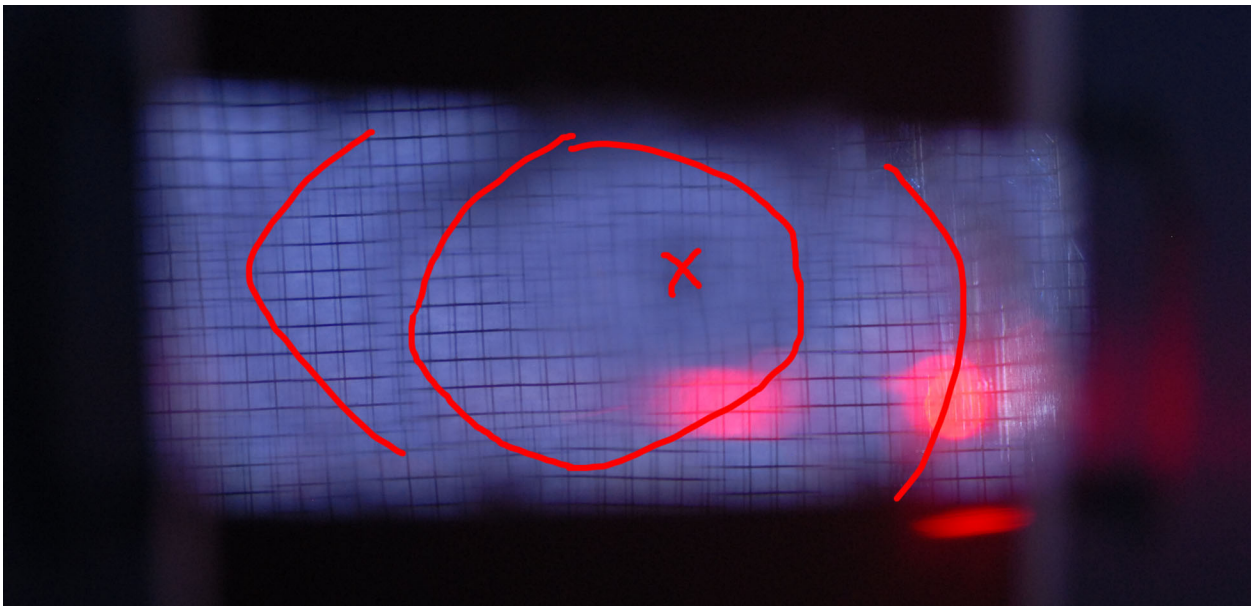

Figure 36: Figure 28 with wave lines added.

In the D200 image we can see that the grid lines are not continuous in many places. Figure 37 has arrows that show some examples of this. When the grid lines are not continuous, this indicates that cracks have started to form, because the glass no longer has a curve that would cause a distorted but continuous line. For this reason, it is apparent that there is so much delay in the sync-and-delay system that we cannot capture the glass deformation before breaking that we successfully captured with the Phantom high-speed video camera.

The main reason we used the D200 was to capture a higher resolution image that is esthetically pleasing. We did succeed in this goal, however we were not able to extract useful data

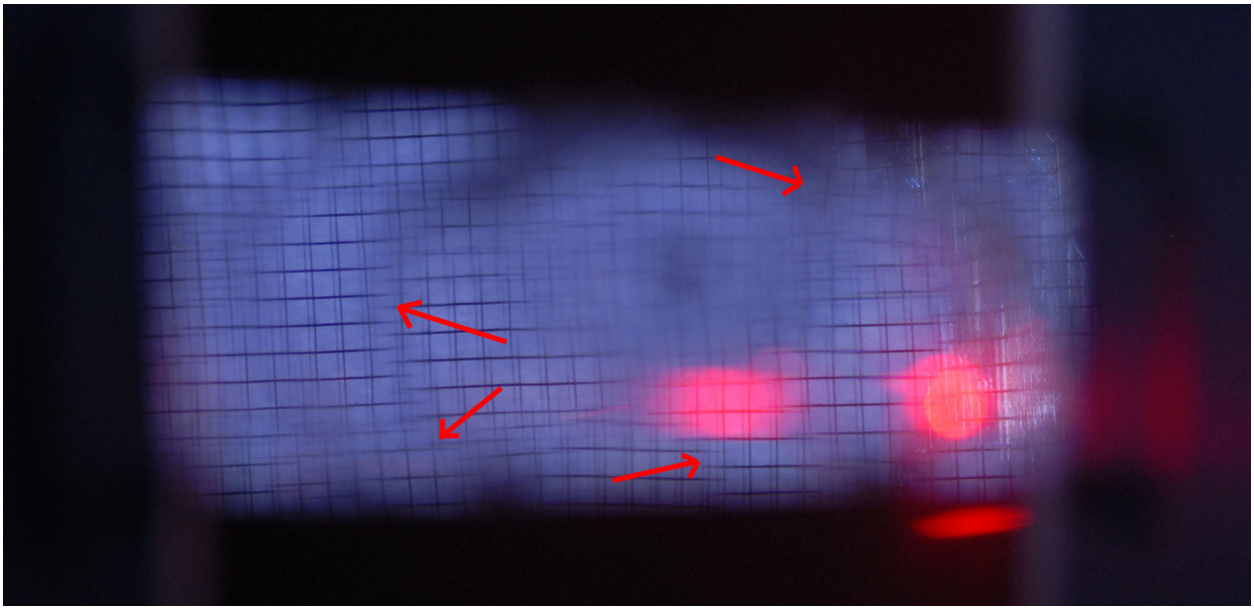

Figure 37: Figure 28 with arrows showing grid line discontinuity. This shows that cracks have already started to form.

from the resulting image. We can see that we can capture higher-resolution images. We can also see that there are circular waves that form on the glass. This is consistent with what we saw on the high-speed video of a BB hitting glass.

5.4 Schlieren Imaging

The Schlieren experiment led us to the conclusion that Schlieren, at least at regular video speeds, does not produce useful data about the process of glass breaking under heat stress. We were ultimately unable to gather any useful data. We did determine that glass does not deform interestingly as it is heated; the glass does not change color in the imager.

Future experiments with Schlieren could try high-speed video. If available, a color high-speed video camera might provide more information about the deformation, because of the importance of hue in Schlieren imaging (hue indicates the direction in which light is being bent).

Additionally, taking Schlieren video of a BB breaking glass could provide useful data. In our other experiments, we found that BBs were more effective than heat expansion at providing both interesting crack patterns and initial glass deformation. BBs travel at a high-enough speed that viewing them with either a high-speed video system or a synch-and-delay system (with a still camera) would produce more-useful data.[2]

[2]Because of resource limitations, we performed the Schlieren experiments without the BB gun while the BB gun was being used for other high-speed video of glass breaking.

A Appendix

References

[2.001] "Mechanics." Course 2.001. Massachusetts Institute of Technology. Spring 2008.

[IM3-JWB] Bales, James W. "Laboratory 3: Multiflash Photography." 6.163 Strobe Project Laboratory. Massachusetts Institute of Technology, Cambridge, MA, 24 September 2008.

[Jones02] Jones, Allison PhD. "Forensic Handbook 2 — Trace Evidence." May 2002. `http://www.channel4.com/science/microsites/S/science/society/forensic_trace.html`. Retrieved 11 Dec 2008.

[Socrate] Socrate, Simona. *A Roadmap to 2.001*, Massachusetts Institute of Technology. p.168. 2007.

[Bhuyan89] Bhuyan, Sanjeeb, Sarah Longenbaker, and Dmitry Portnyagin. *Impacts on Glass — Final Report*. Massachusetts Institute of Technology Strobe Lab (6.163). December 10, 2004.

[Ravi-Chandar] Ravi-Chandar, K. *Dynamic fracture of nominally brittle materials*. International Journal of Fracture 90, 1998.

[Jeronimo] Jeronimo, A. and V. Van Der Haegen. "Schlieren Technique — Lab Notes." EUROAVIA Symposium — Mission to Mars. November 2002. Von Karman Institute for Fluid Dynamics. `http://www.vki.ac.be/event/euroavia/slides/lab1exp.pdf`. Retrieved 12 Dec 2008.

List of Figures

List of Tables

B Point-Capturing App

We developed a simple software tool to speed up the identification of vertex points in an image. The software was quite simple: It loaded an image; then whenever the user clicked on a location in the image, the program would log the location of that click. It accumulated a list of click locations that could be imported into a data analysis program such as Microsoft Excel.
The tool was written as a Web page using HTML augmented with JavaScript. It ran within the Mozilla Firefox 3.0 Web browser.

```
<html>
<head>
<title>Image Pos Calc</title>
<script language="JavaScript">
function onImgClick(event) {
  txt = document.getElementById('text_out');
  txt.value += event.layerX + " " + event.layerY + "\n";
  txt.scrollTop = txt.scrollHeight;
}

function onImgMouseover(event) {
  x = document.getElementById('xcoord');
  y = document.getElementById('ycoord');

  x.innerHTML = String(event.layerX);
  y.innerHTML = String(event.layerY);
}

function updatePhoto() {
  document.getElementById('scan_image').src =
    document.getElementById('target_img_file').value;
}
</script>
</head>
<body style="margin: 0">

<img src="" onclick="onImgClick(event);"
     onmousemove="onImgMouseover(event);" id="scan_image" />
<br />

<label for="target_img_file">Image to View:</label>
<input type="textbox" id="target_img_file" />
<input type="button" value="Update" onclick="updatePhoto();" />
<br />

(<span id="xcoord">0</span>, <span id="ycoord">0</span>)
<br />
<textarea id="text_out" cols="80" rows="24"></textarea>

</body>
</html>
```

C Lab Notes